Elsevier Editorial System(tm) for Journal of Sound and Vibration

Manuscript Draft

Manuscript Number: JSV-D-18-02426R1

Title: DYNAMIC STIFFNESS FORMULATION AND FREE VIBRATION ANALYSIS OF SPECIALLY ORTHOTROPIC MINDLIN PLATES WITH ARBITRARY BOUNDARY CONDITIONS

Article Type: Full Length Article

Section/Category: J Analytical methods and modelling for linear vibration and acoustics

Keywords: free vibration, rectangular orthotropic thick plate, dynamic stiffness method, infinite system of linear equations, arbitrary boundary conditions

Corresponding Author: Professor Stanislav Olegovich Papkov, Ph.D.

Corresponding Author's Institution: Sevastopol State University

First Author: Stanislav Olegovich Papkov, Ph.D.

Order of Authors: Stanislav Olegovich Papkov, Ph.D.; Ranjan Banerjee, Professor

Abstract: A novel dynamic stiffness formulation which includes the effects of shear deformation and rotatory inertia is proposed to carry out the free vibration analysis of thick rectangular orthotropic plates i.e. the formulation is based on an extension of the Mindlin theory to orthotropic plates in a dynamic stiffness context. The modified trigonometric basis is used to construct the general solution for the free vibration problem of the plate in series form, permitting the derivation of an infinite system of linear algebraic equations which connect the Fourier coefficients of the kinematic boundary conditions of its four edges. The boundary conditions are essentially the deflections and angles of rotations constituting the displacement vector and shear forces and bending moments constituting the force vector. The force-displacement relationship is then obtained by relating the two vectors via the dynamic stiffness matrix. Essentially the ensuing infinite system forms the fundamental basis of the paper, which defines the dynamic stiffness matrix for an orthotropic Mindlin plate in an exact sense. Numerical results are obtained by using the Wittrick-Williams algorithm as solution technique. The theory is first validated using published results and then further illustrated by a series of numerical examples. The paper concludes with significant conclusions.

DYNAMIC STIFFNESS FORMULATION AND FREE VIBRATION ANALYSIS OF SPECIALLY ORTHOTROPIC MINDLIN PLATES WITH ARBITRARY BOUNDARY CONDITIONS

S.O. Papkov[a], J.R. Banerjee[b]

[a]Department of Mathematics, Sevastopol State University, Sevastopol

[b]School of Mathematics, Computer Science and Engineering, City, University of London

Abstract

A novel dynamic stiffness formulation which includes the effects of shear deformation and rotatory inertia is proposed to carry out the free vibration analysis of thick rectangular orthotropic plates i.e. the formulation is based on an extension of the Mindlin theory to orthotropic plates in a dynamic stiffness context. The modified trigonometric basis is used to construct the general solution for the free vibration problem of the plate in series form, permitting the derivation of an infinite system of linear algebraic equations which connect the Fourier coefficients of the kinematic boundary conditions of its four edges. The boundary conditions are essentially the deflections and angles of rotations constituting the displacement vector and shear forces and bending moments constituting the force vector. The force-displacement relationship is then obtained by relating the two vectors via the dynamic stiffness matrix. Essentially the ensuing infinite system forms the fundamental basis of the paper, which defines the dynamic stiffness matrix for an orthotropic Mindlin plate in an exact sense. Numerical results are obtained by using the Wittrick-Williams algorithm as solution technique. The theory is first validated using published results and then further illustrated by a series of numerical examples. The paper concludes with significant conclusions.

Keywords: free vibration, rectangular orthotropic thick plate, dynamic stiffness method, infinite system of linear equations, arbitrary boundary conditions

1. Introduction

Free vibration analysis of structures has always been an area of intense research activity, particularly from the point of view of their stability and response characteristics. The subject matter is of considerable importance in aerospace, automobile, construction and ship-building industries, amongst others. It is well recognized that the finite element method (FEM) is a universal tool well-suited to address the problem, particularly in the low and perhaps in the medium frequency range. One of the great advantages of the FEM is, of course, it can handle complex geometries. However, the FEM is understandably an approximate method based on assumed shape functions and therefore, it generally performs poorly in the high frequency range unless exceptionally large number of degrees of freedom utilising high-precision, good quality finite elements are employed. This makes the FEM rather inefficient and computationally expensive in the high frequency range. In many engineering applications, there exists a serious and important need for free vibration analysis in the high frequency range and this need often arises when assessing the flow of vibrational energy in structures, particularly when applying the Statistical Energy Analysis (SEA) method [1, 2]. Investigation of this nature is further stimulated by the fact that the modal density required for the energy flow analysis in structures is usually very high in the high frequency range where the FEM may become inaccurate and unreliable. It should be noted at this stage that there is a powerful alternative to FEM, which does not have such limitations. The alternative is that of the dynamic stiffness method (DSM) which has been described as an exact method in the literature [3, 4]. The DSM is elegant and versatile, and it can be used in a much broader context to analyse the free vibration behaviour of complex structures in all frequency ranges. The DSM is different from the FEM, but it shares many similar features with the FEM. For instance, the DSM has analogous procedure to assemble structural properties of individual structural elements in the same way as the FEM. However, a major difference between the DSM and the FEM arises in that the former is independent of the number of elements used in the analysis and it always gives exact results whereas the latter is mesh dependent and the accuracy of results depends on the number of elements used in the analysis. For instance, one single structural element can used in the DSM to compute any number of natural frequencies without any loss of accuracy which, of course, is impossible in the FEM. The uncompromising accuracy of the DSM stems from the fact that the frequency dependent shape function used to derive the element dynamic stiffness matrix of a structural element originates from the exact solution of the governing differential equation of motion of the element undergoing free vibration. The element dynamic stiffness matrix derived in this way contains both the mass and stiffness properties of the element, unlike the FEM for which the mass and stiffness matrices are always separate and frequency independent, and they are generally derived from chosen shape functions. An outline for the procedure to derive the dynamic stiffness matrix of a structural element can be found in the work of Banerjee [5]. The overall frequency dependent dynamic stiffness matrix of the final structure is obtained by assembling the individual dynamic stiffness matrices of all constituent elements in the structure, in the usual way as in the case of the FEM, but the formulation leads to a non-linear eigenvalue problem and the natural frequencies are generally extracted by applying the

well-known algorithm of Wittrick and Williams [6]. Because of the independency of the accuracy of results on the number of element used in the analysis, the DSM is ideally suited for free vibration analysis in all frequency ranges.

Plate structures are widely used in engineering design. For instance, in the design of an aircraft wing, the top and bottom skins, spar-webs and ribs are often idealized as plate structures for which the free vibration analysis is of great importance and indeed, an essential requirement. Against this background and the DSM being an established and effective tool, which overcomes the shortcomings of the FEM, this paper is set out to investigate the free vibration characteristics of orthotropic Mindlin plates with arbitrary boundary conditions which has not been attempted before. Literature pertaining to the contribution made in this paper is reviewed next.

In most of the papers published to date, the free vibration analysis of plates and plate assemblies using the DSM has been carried out with the assumption that the longitudinal edges of the plates are simply supported, see for example [7-10]. The reason for this can be attributed to the fact that the exact solution is readily available from the theory of elasticity for a simply-supported plate which makes it possible to develop the DSM in an exact sense to compute the natural frequencies and mode shapes of plates and plate assemblies in all frequency ranges. The absence of an exact solution for other types of plate boundary conditions substantially narrowed the range of applicability of the DSM in the past, but this restriction has recently been removed by some outstanding publications in recent years [11-17]. It should be recognized that seeking an exact solution for free vibration of plates with boundary conditions other than the simply-supported one is really very difficult task but, nevertheless, it is necessary because it is a fundamental step to make the DSM development sufficiently general when modelling complex structures. Such a development is of great significance and has far reaching consequences and importantly, it will allow amalgamation of the FEM with the DSM, making a sea change in the simulation based structural analysis and design.

For composite thin rectangular plates new solutions have recently been obtained by Papkov and Banerjee [18] and Papkov [19-20] by applying the superposition method. It was ascertained by them that for a plate which is either clamped or free all-round its four edges, i.e. CCCC and FFFF, respectively, the boundary value problems could be reduced to the regular infinite systems of linear equations. The known law of asymptotic behavior of unique solution for these systems was utilized to construct the dynamic stiffness matrix [11] for free vibration analysis of rectangular thin plates with arbitrary boundary conditions. This approach was later generalized for orthotropic composite thin plates by Liu and Banerjee [12-13]. Within this pretext, the current paper is set out to develop the dynamic stiffness matrix of a thick composite plate by considering the effects of shear deformation and rotatory inertia, i.e. it is for a composite Mindlin plate, and then to apply the ensuing dynamic stiffness matrix to carry out the free vibration analysis with particular reference to the Wittrick-Williams algorithm [6].

The basic theory for thick plates was first developed by Reissner [21] for static problems and then was extended by Mindlin [22] to solve dynamic problems. Following the work of Reissner and Mindlin, exact solutions in the form of trigonometric series were obtained for free vibration and buckling problems of rectangular thick plates only for the case when all or two opposite sides of the plate are simply-supported [23-24]. Investigations about the possibility of achieving exact solutions for other boundary conditions have continued in earnest even to this day. For instance, an attempt to obtain an exact analytical solution for a plate which is clamped all round (CCCC) can be found in the work of Xiang and Liu [25].

A literature review from a sizeable section of published papers reveals that by and large, there are two distinct approaches for free vibration analysis of thick plates which have been adopted by researchers. Both these approaches basically lead to linear algebraic systems of equations. One of them is the well-known Rayleigh-Ritz method and the other is the so-called superposition method. The Rayleigh-Ritz method has been widely used to solve the free vibration problems of thick plates [26, 27]. This method is primarily based on polynomials with properties corresponding to those of the beam functions, see for example, Chung et al. [28] and Chung and Zhou [29] who investigated the free vibration problems of Mindlin plates using the Rayleigh-Ritz method. By contrast, Saha et al [30] used a variational approach when carrying out the free vibration analysis of thick isotropic plates. On the other hand, Xiang et al. [31] used the DSC-Ritz method and solved the problem when the edges of the plate are elastically restrained. The Rayleigh-Ritz method was also used by Liew et al. [32] and Zhou et al. [33] for free vibration analysis of Mindlin plates with elastically restrained edges. However, the method used by Zhou et al. [33] is essentially the superposition method. Their approach for free vibration analysis was extended substantially by Gorman [34] who investigated completely free isotropic plates. Later Gorman [35] used the superposition method for free vibration analysis of point supported Mindlin plates. An important related paper using Levy type solution technique was published by S. D. Yu et al. [36]. It should be noted that in the superposition method, the constructed solution satisfies the governing differential equations exactly but the boundary conditions for forces and displacements are satisfied only approximately, i.e. within the accuracy of solution of the linear system. On the contrary in the Rayleigh-Ritz method, the boundary conditions are satisfied exactly, but the differential equations are satisfied approximately.

In the present paper, a modification of the superposition method is developed for the first time to enable exact solutions for natural vibration of orthotropic thick plates with arbitrary boundary conditions to be made. The proposed approach enhances the superposition method significantly by developing the dynamic stiffness matrix through the process of reducing the boundary value problem to an infinite system of linear algebraic equations. One of the main contributions made in this paper is that the derived infinite system of linear algebraic equations is realised in terms of boundary displacements and boundary forces. Accordingly, the dynamic stiffness matrix of an orthotropic Mindlin plate is formulated and it

comes into effect to enable free vibration analysis of orthotropic Mindlin plates and plate assemblies to be made.

The dynamic stiffness theory is systematically developed and demonstrated by results computed for a carefully selected sample of illustrative examples. Some of the results are compared with published ones. The results from the present theory, being exact, to all intent and purposes, and therefore, provide benchmark solutions which can be used as an aid to validate the finite element and other approximate methods when carrying out the free vibration analysis of Mindlin orthotropic plates with any arbitrary boundary conditions. For results corresponding to all of the boundary conditions reported for an individual orthotropic Mindlin plate, it has been possible to obtain an explicit analytical series solution to arrive at the frequency equations, but the dynamic stiffness matrix developed is enormously more significant because such a development has a much wider applicability to analyse complex structures comprising Mindlin plate assemblies.

2. Governing differential equations and general solutions

Figure 1 shows schematically in a right-handed rectangular Cartesian coordinate system the distributions of forces (Fig 1a) and displacements (Fig. 1b) of a thick orthotropic Mindlin plate of thickness h, and sides $2a$ and $2b$, which are respectively the length and breadth of the plate. The plane of symmetry is perpendicular to the Z-axis. The elastic constants needed to define the properties of the Mindlin plate are in the usual notation the Young's modulus E_1 and E_2 in the X and Y directions, the shear moduli G_{12}, G_{13} and G_{23} in the XY, XZ and YZ planes and the major and minor Poisson's ratios ν_{12} and ν_{21}, respectively. (Note that ν_{12} and ν_{21} are related to each other by the relationship $\nu_{12}/\nu_{21}=E_1/E_2$.)

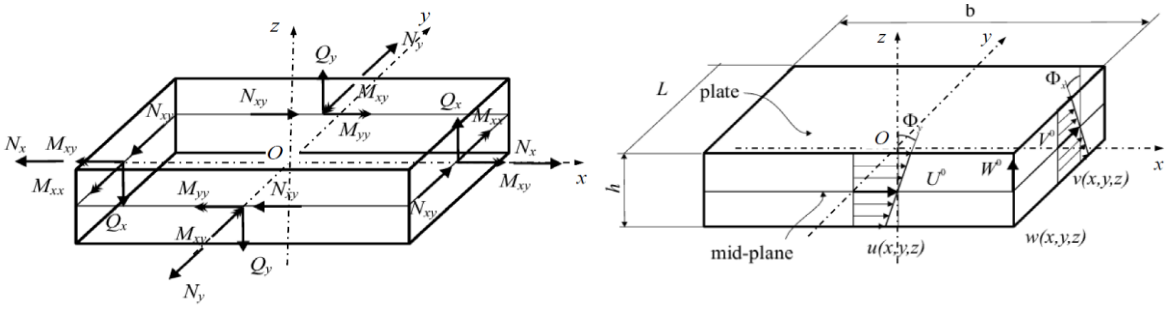

(a) Forces (b) Displacements

Fig.1. In-plane and out-of-plane forces and displacements of a Mindlin plate element

Referring to Fig.1 the displacements field of the plate in the usual notation can be written as [21, 22]

$$U(x,y,z,t) = u^0(x,y,t) - z\phi_y^0(x,y,t), \quad V(x,y,z,t) = v^0(x,y,t) - z\phi_x^0(x,y,t),$$

$$W(x,y,z,t) = w^0(x,y,t) \tag{1}$$

As in the case of the Timoshenko beam theory, the Mindlin plate theory proposes that the cross-section through the thickness of the plate remains straight, but not normal to the plate middle-surface due to effects of the shear deformation. This proposition is a significant improvement of the classical theory and it basically leads to two rotational degrees of freedom which are essentially the bending rotations of the plate cross-section about the X and Y axes, respectively, i.e. ϕ_x^0 and ϕ_y^0 that are independent of the first derivative of the bending displacements with respect to *x* and *y*, unlike the assumptions made in the classical plate theory.

The bending moments, twisting moments and shear forces per unit length, acting on an orthotropic plate can be expressed in the usual notation as

$$\left.\begin{aligned} &M_x = -D_{11}\frac{\partial \phi_y^0}{\partial x} - D_{12}\frac{\partial \phi_x^0}{\partial y}; \quad M_y = -D_{12}\frac{\partial \phi_y^0}{\partial x} - D_{22}\frac{\partial \phi_x^0}{\partial y}; \quad M_{xy} = -D_{66}\left(\frac{\partial \phi_y^0}{\partial y} + \frac{\partial \phi_x^0}{\partial x}\right) \\ &Q_x = A_{44}\left(\frac{\partial w^0}{\partial x} - \phi_y^0\right); \quad Q_y = A_{55}\left(\frac{\partial w^0}{\partial y} - \phi_x^0\right) \end{aligned}\right\} \tag{2}$$

where $D_{11}, D_{22}, D_{12}, D_{66}, A_{44}$ and A_{55} are the elements of the **D** and **A** matrices obtained from the classical orthotropic plate theory as given below with κ being the shear correction factor which accounts for the non-uniform shear stress distribution through the thickness of the plate.

$$D_{11} = \frac{h^3 E_1}{12(1-\nu_{12}\nu_{21})}; D_{22} = \frac{h^3 E_2}{12(1-\nu_{12}\nu_{21})}; D_{12} = \frac{h^3 \nu_{12} E_2}{12(1-\nu_{12}\nu_{21})}; D_{66} = \frac{h^3 G_{12}}{12}; A_{44} = \kappa h G_{13}; A_{55} = \kappa h G_{23} \tag{3}$$

In terms of the bending moments, twisting moments and shear forces per unit length, the governing differential equations of free vibration for an orthotropic Mindlin plate have the same form as that of its isotropic counterpart which can be written as [22]

$$\left.\begin{aligned} &\frac{\partial M_x}{\partial x} + \frac{\partial M_{xy}}{\partial y} - Q_x = -\frac{\rho h^3}{12}\frac{\mathrm{d}^2 \phi_y^0}{dt^2} \\ &\frac{\partial M_{xy}}{\partial x} + \frac{\partial M_y}{\partial y} - Q_y = -\frac{\rho h^3}{12}\frac{\mathrm{d}^2 \phi_x^0}{dt^2} \\ &\frac{\partial Q_x}{\partial x} + \frac{\partial Q_y}{\partial y} = \rho h \frac{\mathrm{d}^2 w^0}{dt^2} \end{aligned}\right\} \tag{4}$$

For harmonic oscillation, i.e. when $\phi_x^0(x,y,t) = \phi_x(x,y)\mathrm{e}^{i\omega t}, \phi_y^0(x,y,t) = \phi_y(x,y)\mathrm{e}^{i\omega t}$ and $w^0(x,y,t) = W(x,y)\mathrm{e}^{i\omega t}$, Eqs. (2) with the help of Eqs. (4) lead to the following three differential equations

$$\left.\begin{aligned}
&\frac{\partial^2\phi_y}{\partial x^2}+k_6\frac{\partial^2\phi_y}{\partial y^2}+\tilde{k}\frac{\partial^2\phi_x}{\partial x\partial y}+k_4\left(\frac{\partial W}{\partial x}-\phi_y\right)+\Omega_h^4\phi_y=0\\
&k_2\frac{\partial^2\phi_x}{\partial y^2}+k_6\frac{\partial^2\phi_x}{\partial x^2}+\tilde{k}\frac{\partial^2\phi_y}{\partial x\partial y}+k_5\left(\frac{\partial W}{\partial y}-\phi_x\right)+\Omega_h^4\phi_x=0\\
&k_4\left(\frac{\partial^2 W}{\partial x^2}-\frac{\partial\phi_y}{\partial x}\right)+k_5\left(\frac{\partial^2 W}{\partial y^2}-\frac{\partial\phi_x}{\partial y}\right)+\Omega^4 W=0
\end{aligned}\right\} \tag{5}$$

where

$$\left.\begin{aligned}
&\Omega^4=\frac{\rho h\omega^2}{D_{11}},\quad \Omega_h^4=\frac{h^2}{12}\Omega^4\\
&k_2=\frac{D_{22}}{D_{11}},\quad k_4=\frac{A_{44}}{D_{11}},\quad k_5=\frac{A_{55}}{D_{11}},\quad k_6=\frac{D_{66}}{D_{11}},\quad \tilde{k}=\frac{D_{66}+D_{12}}{D_{11}}
\end{aligned}\right\} \tag{6}$$

In order to facilitate the analytical derivations, a unified notation using *k* and *j* where each of *k* and *j* can be either 0 or 1 is used to represent the displacements field so that W, ϕ_x and ϕ_y can be described in the form of the sum of four sub-components of even and odd functions depending on the values of *k* and *j* with the understanding that 0 denotes an even function whereas 1 denotes an odd function. This approach which will be clearer later, is analogous to the one proposed by Papkov and Banerjee [18] earlier when they carried out the free vibration analysis of thin orthotropic plates. It should be noted, that it is possible to define any arbitrary asymmetric motion of the rectangular plate of Fig. 1 by using only one quarter of the plate and taking full advantage of its symmetry about the planes through its mid-point. In this respect, the indices *k* and *j* denote symmetric and anti-symmetric boundary conditions relating to XZ and YZ planes, respectively. The symmetry reduces the size of the problem, but appropriate boundary conditions for displacements and forces must be applied on the enforced plane of symmetry. Clearly there is no approximation involved in the process. In terms of the indices *k* and *j*, the pair (*k*, *j*) indicates any of the four component cases of the quarter plate lying in the positive XY quadrant of Fig. 1(a), depending on the values of *k* and *j* each of which can be either 0 and 1. Thus, (0,0), (0,1), (1,1) and (1,0) represent symmetric-symmetric, symmetric-anti-symmetric, anti-symmetric-antisymmetric and anti-symmetric-symmetric boundary conditions of the displacement and forces about the XZ and YZ planes, respectively.

In this way, the displacements W, ϕ_x and ϕ_y can be represented as follows

$$\begin{pmatrix} W\\ \phi_x\\ \phi_y\end{pmatrix}=\sum_{k,j=0}^{1}\begin{pmatrix} W_{kj}\\ \phi_{x,kj}\\ \phi_{y,kj}\end{pmatrix} \tag{7}$$

Completeness of the general solution at the boundaries $x=\pm a$ and $y=\pm b$ (see Fig. 1) can be provided if each sub-component of the displacements W_{kj}, $\phi_{x,kj}$ and $\phi_{y,kj}$ is constructed in the form of the sum of two Fourier series shown below

$$W_{kj} = W_{kj}^{(1)} + W_{kj}^{(2)}, \quad \phi_{x,kj} = \phi_{x,kj}^{(1)} + \phi_{x,kj}^{(2)}, \quad \phi_{y,kj} = \phi_{y,kj}^{(1)} + \phi_{y,kj}^{(2)} \tag{8}$$

where first term indicated by (1) in Eqs. (8) corresponds to Fourier series in the X direction whereas the second term indicated by (2) corresponds to Fourier series in the Y direction.

For simplicity and ease of presentation, the following notation for trigonometric and hyperbolic functions is introduced [18-20].

$$H_0 = \cosh(z), \; H_1 = \sinh(z), \; T_0 = \cos(z), \; T_1 = \sin(z). \tag{9}$$

Then the terms of first series in Eq. (8) can be written in the form

$$W_{kj}^{(1)} = AH_j(py)T_k(\alpha x), \quad \phi_{y,kj}^{(1)} = BH_j(py)T_k'(\alpha x), \quad \phi_{x,kj}^{(1)} = CH_j'(py)T_k(\alpha x) \tag{10}$$

where *A*, *B* and *C* are respectively the amplitudes of bending displacement and bending rotations, α is a constant of separation and *p* is a characteristic parameter.

Substituting Eqs. (10) into the system of Eqs. (5), the following system of algebraic equations are obtained

$$\left.\begin{aligned} &\alpha k_4 A + \left(k_6 p^2 - \alpha^2 - k_4 + \Omega_h^4\right)B + \alpha p\tilde{k} C = 0 \\ &p k_5 A - \alpha p\tilde{k} B + \left(k_2 p^2 - k_6\alpha^2 - k_5 + \Omega_h^4\right)C = 0 \\ &\left(k_5 p^2 - k_4\alpha^2 + \Omega^4\right)A + \alpha k_4 B - p k_5 C = 0 \end{aligned}\right\} \tag{11}$$

Quite obviously, the Eqs. (11) will have a non-trivial solution for *A*, *B*, and *C* if the determinant formed by the coefficients of *A*, *B*, and *C* of Eqs. (11) is set to zero. This leads to the following characteristic equation in *p*.

$$\det\begin{pmatrix} \alpha k_4 & k_6 p^2 - \alpha^2 - k_4 + \Omega_h^4 & \alpha p\tilde{k} \\ p k_5 & -\alpha p\tilde{k} & k_2 p^2 - k_6\alpha^2 - k_5 + \Omega_h^4 \\ k_5 p^2 - k_4\alpha^2 + \Omega^4 & \alpha k_4 & -p k_5 \end{pmatrix} = 0 \tag{12}$$

By expanding the determinant of Eq, (12) and making substantial algebraic manipulation, the following characteristic or auxiliary equation is obtained

$$c_0 p^6 + c_1 p^4 + c_2 p^2 + c_3 = 0 \tag{13}$$

where

$$c_0 = k_2 k_5 k_6\,, \tag{14}$$

$$c_1 = \alpha^2\left(k_5\left(\tilde{k}^2 - k_6^2 - k_2\right) - k_2 k_4 k_6\right) + \Omega_h^4 k_5\left(k_2 + k_6\right) + \Omega^4 k_2 k_6 - k_2 k_4 k_5\,, \tag{15}$$

$$\begin{aligned} c_2 = {} & \alpha^4\left(k_4\left(k_2 + k_6^2 - \tilde{k}^2\right) + k_5 k_6\right) + \alpha^2\left(\Omega^4\left(\tilde{k}^2 - k_6^2\right) - k_5\Omega_h^4\left(1 + k_6\right) - k_2\left(\Omega^4 + k_4\Omega_h^4\right) + \right. \\ & \left. + k_4\left(2k_5\left(k_6 + \tilde{k}\right) - k_6\Omega_h^4\right)\right) + \Omega^4\left(\Omega_h^4\left(k_2 + k_6\right) - k_2 k_4\right) + k_5\left(\Omega_h^4\left(\Omega_h^4 - k_4\right) - k_6\Omega^4\right), \end{aligned} \tag{16}$$

$$\begin{aligned} c_3 = {} & -\alpha^6 k_4 k_6 + \alpha^4\left(-k_4 k_5 + k_6\Omega^4 + k_4\Omega_h^4\left(1 + k_6\right)\right) + \alpha^2\left(\Omega^4\left(k_5 + k_4 k_6 - \Omega_h^4\right) + \right. \\ & \left. + \Omega_h^4\left(k_4 k_5 - k_6\Omega^4 - k_4\Omega_h^4\right)\right) + \Omega^4\left(\Omega_h^4 - k_4\right)\left(\Omega_h^4 - k_5\right). \end{aligned} \tag{17}$$

The characteristic equation (13) is a cubic in p^2 with associated roots $p_1^2(\alpha), p_2^2(\alpha)$ and $p_3^2(\alpha)$. These roots can be expressed in analytical forms with help of Cordano formulas [37] as

$$p_1(\alpha) = \sqrt{\xi^+ + \xi^- - \frac{c_1}{3c_0}}\,; \qquad p_{2,3}(\alpha) = \sqrt{-\frac{\xi^+ + \xi^-}{2} - \frac{c_1}{3c_0} \pm \frac{i\sqrt{3}}{2}\left(\xi^+ - \xi^-\right)} \tag{18}$$

where

$$\xi^{\pm} = \sqrt[3]{r_p \pm \sqrt{r_p^2 + s_p^3}}\,;\; r_p = \frac{c_1 c_2}{6c_0^2} - \frac{c_3}{2c_0} - \frac{c_1^3}{27c_0^3};\quad s_p = \frac{c_2}{3c_0} - \frac{c_1^2}{9c_0^2}\,. \tag{19}$$

Then choosing one of values *A*, *B* and *C* to be an arbitrary constant, for example $C = 1$, we obtain the following solution of system of Eqs. (11)

$$\left.\begin{aligned} A_l(\alpha) &= \frac{\tilde{k}k_5 p_l^2 - k_4\left(k_2 p_l^2 - k_6\alpha^2 - k_5 + \Omega_h^4\right)}{p_l\left(\tilde{k}k_5 p_l^2 - \tilde{k}k_4\alpha^2 + k_4 k_5 + \tilde{k}\Omega^4\right)} \\ B_l(\alpha) &= \frac{k_5^2 p_l^2 + \left(k_2 p_l^2 - k_6\alpha^2 - k_5 + \Omega_h^4\right)\left(k_5 p_l^2 - k_4\alpha^2 + \Omega^4\right)}{\alpha p_l\left(\tilde{k}k_5 p_l^2 - \tilde{k}k_4\alpha^2 + k_4 k_5 + \tilde{k}\Omega^4\right)} \end{aligned}\right\}; \tag{20}$$

In the special case when the separation constant $\alpha = 0$ then particular solution of Eqs. (5) will be functions of *y* only. For this special case, one can write the solution in the following form

$$W_{kj}^{(1)} = AH_j(p_0 y); \quad \phi_{y,kj}^{(1)} = 0; \quad \phi_{x,kj}^{(1)} = H_j'(p_0 y) \tag{21}$$

Substituting Eqs. (21) into Eqs. (5) gives the following linear relationship for *A* is obtained

$$\left.\begin{aligned} & p_0 k_5 A + \left(k_2 p_0^2 - k_5 + \Omega_h^4\right) = 0 \\ & \left(k_5 p_0^2 + \Omega^4\right)A - p_0 k_5 = 0 \end{aligned}\right\} \tag{22}$$

Expressing the coefficient *A* from both the relationships of Eqs. (22), one can write the characteristic equation for $\alpha = 0$ as

$$k_2 k_5 p_0^4 + \left(k_2\Omega^4 + k_5\Omega_h^4\right)p_0^2 + \Omega^4\left(\Omega_h^4 - k_5\right) = 0\,, \tag{23}$$

Equation (23) is quadratic in p_0^2, and therefore the four roots of Eq. (23) can be expressed in the following analytical form

$$p_{l,0k} = \sqrt{\frac{-\left(\Omega^4 k_2 + \Omega_h^4 k_5\right) \pm \sqrt{\left(\Omega^4 k_2 + \Omega_h^4 k_5\right)^2 + 4k_2 k_5^2 \Omega^4}}{2k_2 k_5}} \tag{24}$$

where the suffix l can be 1 or 2 with l = 1 corresponds to + and l = 2 corresponds to – before the inner square root sign of in Eq. (24).

Proceeding in this way, it is possible to generate the indefinite coefficients from Eqs. (21) as follows

$$A_{l,0k} = \frac{k_5 p_{l,0k}}{k_5 p_{l,0k}^2 + \Omega^4} \qquad (l = 1, 2) \tag{25}$$

Thus the analytical solution for the first term of Eqs. (8) derived by Fourier series in terms of the variable x is now available.

Proceeding in a similar manner and treating Eqs. (10)-(25) in an analogous manner, the terms of the second series in Eq. (8) can be obtained in the following form

$$W_{kj}^{(2)} = E\,H_k(qx)T_j(\beta y), \quad \phi_{y,kj}^{(2)} = F\,H_k'(qx)T_j(\beta y), \quad \phi_{x,kj}^{(2)} = G\,H_k(qx)T_j'(\beta y) \tag{26}$$

For this case, the following system of algebraic equations are derived

$$\left.\begin{aligned} &qk_4 E + \left(q^2 - k_6\beta^2 - k_4 + \Omega_h^4\right)F - q\beta\tilde{k}G = 0 \\ &\beta k_5 E + q\beta\tilde{k}F + \left(k_6 q^2 - k_2\beta^2 - k_5 + \Omega_h^4\right)G = 0 \\ &\left(k_4 q^2 - k_5\beta^2 + \Omega^4\right)E - qk_4 F + \beta k_5 G = 0 \end{aligned}\right\} \tag{27}$$

Setting the determinant formed by the coefficients of E, F and G of Eqs. (27) to zero, gives the following characteristic equation in terms of q

$$d_0 q^6 + d_1 q^4 + d_2 q^2 + d_3 = 0 \tag{28}$$

where

$$d_0 = k_4 k_6, \tag{29}$$

$$d_1 = \beta^2\left(k_4\left(\tilde{k}^2 - k_6^2 - k_2\right) - k_5 k_6\right) + \Omega_h^4 k_4\left(1 + k_6\right) + \Omega^4 k_6 - k_4 k_5, \tag{30}$$

$$\begin{aligned} d_2 = {} & \beta^4\left(k_5\left(k_2 + k_6^2 - \tilde{k}^2\right) + k_2 k_4 k_6\right) + \beta^2\left(2k_4 k_5\left(k_6 + \tilde{k}\right) - \Omega^4\left(k_2 + k_6^2 - \tilde{k}^2\right) - \right. \\ & \left. - \Omega_h^4\left(k_2 k_4 + k_5 + k_4 k_6 + k_5 k_6\right)\right) + \Omega^4\left(\Omega_h^4\left(1 + k_6\right) - k_5 - k_4 k_6\right) + k_4\Omega_h^4\left(\Omega_h^4 - k_5\right), \end{aligned} \tag{31}$$

$$\begin{aligned} d_3 = {} & -\beta^6 k_2 k_5 k_6 + \beta^4\left(-k_2 k_4 k_5 + k_2 k_6\Omega^4 + k_5\Omega_h^4\left(k_2 + k_6\right)\right) + \beta^2\left(\Omega^4\left(k_2 k_4 + k_5 k_6 - k_2\Omega_h^4\right) + \right. \\ & \left. + \Omega_h^4\left(k_4 k_5 - k_6\Omega^4 - k_5\Omega_h^4\right)\right) + \Omega^4\left(\Omega_h^4 - k_4\right)\left(\Omega_h^4 - k_5\right). \end{aligned} \tag{32}$$

The sixth order polynomial of Eq. (28) can be reduced to a cubic and by taking the square root of the roots of the cubic equation so that it is possible to obtain all the six roots of Eq. (28) as follows

$$q_1(\beta) = \sqrt{\eta^+ + \eta^- - \frac{d_1}{3d_0}}\ ;\ q_{2,3}(\beta) = \sqrt{-\frac{\eta^+ + \eta^-}{2} - \frac{d_1}{3d_0} \pm \frac{i\sqrt{3}}{2}\left(\eta^+ - \eta^-\right)} \tag{33}$$

where

$$\eta^{\pm} = \sqrt[3]{r_q \pm \sqrt{r_q^2 + s_q^3}}\ ;\ r_q = \frac{d_1 d_2}{6d_0^2} - \frac{d_3}{2d_0} - \frac{d_1^3}{27d_0^3};\quad s_q = \frac{d_2}{3d_0} - \frac{d_1^2}{9d_0^2}\,. \tag{34}$$

Now setting $F = 1$, the coefficients in Eqs. (26) can be expressed as

$$\left.\begin{aligned} E_l(\beta) &= \frac{\tilde{k}k_4 q_l^2 - k_5\left(q_l^2 - k_6\beta^2 - k_4 + \Omega_h^4\right)}{q_l\left(\tilde{k}k_4 q_l^2 - \tilde{k}k_5\beta^2 + k_4k_5 + \tilde{k}\Omega^4\right)} \\ G_l(\alpha) &= \frac{k_4^2 q_l^2 + \left(q_l^2 - k_6\beta^2 - k_4 + \Omega_h^4\right)\left(k_4 q_l^2 - k_5\beta^2 + \Omega^4\right)}{q_l\beta\left(\tilde{k}k_4 q_l^2 - \tilde{k}k_5\beta^2 + k_4k_5 + \tilde{k}\Omega^4\right)} \end{aligned}\right\} \tag{35}$$

For the case when the separation constant $\beta = 0$ the solution can be sought in the following form

$$W_{kj}^{(2)} = E\,H_k(q_0 x);\quad \phi_{y,kj}^{(2)} = H_k'(q_0 x);\quad \phi_{x,kj}^{(2)} = 0 \tag{36}$$

In similar manner as before, by substituting Eqs. (36) into Eqs. (5) one can obtain the characteristic equation for $\beta = 0$ as

$$k_4 q_0^4 + \left(\Omega^4 + k_4\Omega_h^4\right)q_0^2 + \Omega^4\left(\Omega_h^4 - k_4\right) = 0\,, \tag{37}$$

Equation (35) is quadratic in q_0^2 and the four roots of the quartic can be expressed in analytical form as follows

$$q_{l,0j} = \sqrt{\frac{-\left(\Omega^4 + \Omega_h^4 k_4\right) \pm \sqrt{\left(\Omega^4 + \Omega_h^4 k_4\right)^2 + 4k_4^2\Omega^4}}{2k_4}} \tag{38}$$

where the suffix l can be 1 or 2 with $l = 1$ corresponds to the solution with + sign and $l = 2$ corresponds to - sign before the inner square root sign of Eq. (38).

The values of indefinite coefficients can now be derived as

$$E_{l,0j} = \frac{k_4 q_{l,0j}}{k_4 q_{l,0j}^2 + \Omega^4} \qquad (l = 1, 2) \tag{39}$$

Equations (26) to (39) enable one to construct the second terms of the analytical solution represented by Eqs. (8) in the form of Fourier series of variable y.

It should be noted that each term in Eq. (10), Eq. (21), Eq. (26) and Eq. (36) satisfies the governing system of differential equations of Eqs. (5) for any values of the constants of separation α or β. However, if we choose these constants as

$$\alpha_{nk}=\frac{\pi}{a}\left(n-\frac{k}{2}\right)=\begin{cases}\dfrac{\pi n}{a}, & k=0\\ \dfrac{\pi(2n-1)}{2a}, & k=1\end{cases};\quad \beta_{nj}=\frac{\pi}{b}\left(n-\frac{j}{2}\right)=\begin{cases}\dfrac{\pi n}{b}, & j=0\\ \dfrac{\pi(2n-1)}{2b}, & j=1\end{cases} \tag{40}$$

then the solution can be expressed in the form of classical Fourier series at the boundaries of plate.

With the help of Eqs. (40) one can denote the roots and associated coefficients in more simple way as follows

$$p_l(\alpha_{nk})=p_{l,nk},\ q_l(\beta_{nj})=q_{l,nj},\ A_l(\alpha_{nk})=A_{l,nk}\ \text{ etc.} \tag{41}$$

Summarizing all the above terms of Eqs. (10), (21), (26), (36) with arbitrary coefficients X_{10}, X_{20}, X_{ln} and Y_{10}, Y_{20}, Y_{ln} ($l=1,2,3;\ n=1,2,...$) it is now possible to write the general solution of Eqs. (5) in the form of infinite series as follows

$$W_{kj}=\delta_{k0}\left(X_{10}A_{1,0k}H_j(p_{1,0k}y)+X_{20}A_{2,0k}H_j(p_{2,0k}y)\right)+\delta_{j0}\left(Y_{10}E_{1,0j}H_k(q_{1,0j}x)+Y_{20}E_{2,0j}H_k(q_{2,0j}x)\right)+$$
$$+\sum_{n=1}^{\infty}\sum_{l=1}^{3}X_{ln}A_{l,nk}H_j(p_{l,nk}y)T_k(\alpha_{nk}x)+\sum_{n=1}^{\infty}\sum_{l=1}^{3}Y_{ln}E_{l,nj}H_k(q_{l,nj}x)T_j(\beta_{nj}y); \tag{42}$$

$$\phi_{y,kj}=\delta_{j0}\left(Y_{10}H_k'(q_{1,0j}x)+Y_{20}H_k'(q_{2,0j}x)\right)+\sum_{n=1}^{\infty}\sum_{l=1}^{3}X_{ln}B_{l,nk}H_j(p_{l,nk}y)T_k'(\alpha_{nk}x)+\sum_{n=1}^{\infty}\sum_{l=1}^{3}Y_{ln}H_k'(q_{l,nj}x)T_j(\beta_{nj}y) \tag{43}$$

$$\phi_{x,kj}=\delta_{k0}\left(X_{10}H_j'(p_{1,0k}y)+X_{20}H_j'(p_{2,0k}y)\right)+\sum_{n=1}^{\infty}\sum_{l=1}^{3}X_{ln}H_j'(p_{l,nk}y)T_k(\alpha_{nk}x)+\sum_{n=1}^{\infty}\sum_{l=1}^{3}Y_{ln}G_{l,nj}H_k(q_{l,nj}x)T_j'(\beta_{nj}y) \tag{44}$$

Here the absence of constant term in the odd expansion can be written with the help of Kronecker delta δ_{kn} together with the above mentioned arbitrary coefficients.

3. Formulation of the dynamic stiffness matrix

Figure 2 shows the plan view of the rectangular plate together with the amplitudes of the forces and displacements at the boundaries of the plate. The development of the dynamic stiffness matrix constitutes the establishment of the relationship between the amplitudes of the forces to those of the displacements on the four sides of the plate.

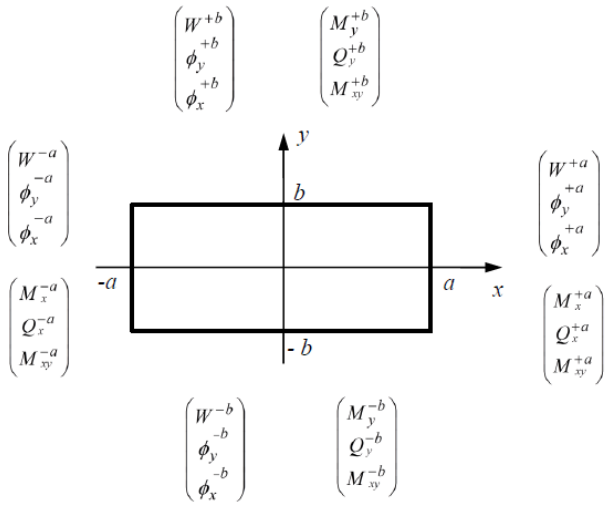

Fig.2. Plan view and boundary conditions for the amplitudes of forces and displacements of the plate

On numerous occasions, the dynamic stiffness method has been applied to Levy-type rectangular plates for which one pair of opposite edges are simply supported [6-10]. In the case of such simply supported boundary conditions, it is possible to express an explicit dependence between boundary values of displacements and boundary values of forces for each mode of vibration because the mode shapes can be represented by sine waves. For other boundary conditions the dynamic stiffness method can be applied with some difficulty. However, the dynamic stiffness matrix formulation for an individual plate element can be based on the same idea used for the simply supported plates. What is essentially required is the appropriate substitution of the boundary conditions for displacements and forces into the general solution and then elimination of the arbitrary constants which establishes the force-displacement relationship at the boundaries of the plate via the frequency-dependent dynamic stiffness matrix [11-12]. Although the formulation of the dynamic stiffness matrix for the general case when the plate is completely free at all its edges is much more difficult that the simply supported Levy type of plates, from a conceptual point of view, the central procedure to connect the force vector to the corresponding displacement vector is essentially the same, as explained below.

Let the boundary components of displacements and forces at the boundaries of the plate (see Fig. 2) can be represented by trigonometric series as follows.

$$
\left.
\begin{aligned}
d^{\pm a} &= \begin{pmatrix} W^{\pm a} \\ \phi_y^{\pm a} \\ \phi_x^{\pm a} \end{pmatrix} = \begin{pmatrix} W_0^{\pm a} \\ \phi_{y0}^{\pm a} \\ \phi_{x0}^{\pm a} \end{pmatrix} + \sum_{m=1}^{\infty} \begin{pmatrix} W_m^{\pm a,0} \\ \phi_{ym}^{\pm a,0} \\ \phi_{xm}^{\pm a,0} \end{pmatrix} T_0(\beta_{m0} y) + \sum_{m=1}^{\infty} \begin{pmatrix} W_m^{\pm a,1} \\ \phi_{ym}^{\pm a,1} \\ \phi_{xm}^{\pm a,1} \end{pmatrix} T_1(\beta_{m1} y) \\
f^{\pm a} &= \frac{1}{D_{11}} \begin{pmatrix} -M_x^{\pm a} \\ Q_x^{\pm a} \\ -M_{xy}^{\pm a} \end{pmatrix} = \begin{pmatrix} M_{x0}^{\pm a} \\ Q_{x0}^{\pm a} \\ M_{xy0}^{\pm a} \end{pmatrix} + \sum_{m=1}^{\infty} \begin{pmatrix} M_{xm}^{\pm a,0} \\ Q_{xm}^{\pm a,0} \\ M_{xym}^{\pm a,0} \end{pmatrix} T_0(\beta_{m0} y) + \sum_{m=1}^{\infty} \begin{pmatrix} M_{xm}^{\pm a,0} \\ Q_{xm}^{\pm a,0} \\ M_{xym}^{\pm a,0} \end{pmatrix} T_1(\beta_{m1} y) \\
d^{\pm b} &= \begin{pmatrix} W^{\pm b} \\ \phi_y^{\pm b} \\ \phi_x^{\pm b} \end{pmatrix} = \begin{pmatrix} W_0^{\pm b} \\ \phi_{y0}^{\pm b} \\ \phi_{x0}^{\pm b} \end{pmatrix} + \sum_{m=1}^{\infty} \begin{pmatrix} W_m^{\pm b,0} \\ \phi_{ym}^{\pm b,0} \\ \phi_{xm}^{\pm b,0} \end{pmatrix} T_0(\alpha_{m0} x) + \sum_{m=1}^{\infty} \begin{pmatrix} W_m^{\pm b,1} \\ \phi_{ym}^{\pm b,1} \\ \phi_{xm}^{\pm b,1} \end{pmatrix} T_1(\alpha_{m1} x) \\
f^{\pm b} &= \frac{1}{D_{11}} \begin{pmatrix} -M_y^{\pm b} \\ Q_y^{\pm b} \\ -M_{xy}^{\pm b} \end{pmatrix} = \begin{pmatrix} M_{y0}^{\pm b} \\ Q_{y0}^{\pm b} \\ M_{xy0}^{\pm b} \end{pmatrix} + \sum_{m=1}^{\infty} \begin{pmatrix} M_{ym}^{\pm b,0} \\ Q_{ym}^{\pm b,0} \\ M_{xym}^{\pm b,0} \end{pmatrix} T_0(\alpha_{m0} x) + \sum_{m=1}^{\infty} \begin{pmatrix} M_{ym}^{\pm b,1} \\ Q_{ym}^{\pm b,1} \\ M_{xym}^{\pm b,1} \end{pmatrix} T_1(\alpha_{m1} x)
\end{aligned}
\right\} \qquad (45)
$$

Due to the properties of the trigonometric series with basis $\left\{1, \cos\frac{\pi m t}{T}, \sin\frac{\pi(m-1/2)t}{T}\right\}$ when $t \in [-T;T]$, any prescribed classical boundary conditions can be expressed according to Eqs. (45). Furthermore, the boundary conditions of any arbitrary form can also be represented as the sum of four boundary conditions with a given symmetry along the coordinate axes. It can be accomplished by selecting the even and odd components of the boundary conditions of the general form Eqs. (45).

In view of Eqs. (2), the general solution given by Eqs. (42)-(44) enables one to derive expressions of force components for each of the component cases of symmetry as follows.

$$
-\frac{M_{x,kj}}{D_{11}} = k^* \delta_{k0} \left(X_{10} p_{1,0k} H_j(p_{1,0k} y) + X_{20} p_{2,0k} H_j(p_{2,0k} y) \right) + \delta_{j0} \left(Y_{10} q_{1,0\,j} H_k(q_{1,0\,j} x) + Y_{20} q_{1,0\,j} H_k(q_{2,0\,j} x) \right) +
$$

$$
+ \sum_{n=1}^{\infty} \sum_{l=1}^{3} X_{ln} \left(k^* p_{l,nk} - \alpha_{nk} B_{l,nk} \right) H_j(p_{l,nk} y) T_k(\alpha_{nk} x) + \sum_{n=1}^{\infty} \sum_{l=1}^{3} Y_{ln} \left(q_{l,nj} - k^* \beta_{nj} G_{l,nj} \right) H_k(q_{l,nj} x) T_j(\beta_{nj} y); \qquad (46)
$$

$$
-\frac{M_{y,kj}}{D_{11}} = k_2 \delta_{k0} \left(X_{10} p_{1,0k} H_j(p_{1,0k} y) + X_{20} p_{2,0k} H_j(p_{2,0k} y) \right) + \delta_{j0} k^* \left(Y_{10} q_{1,0\,j} H_k(q_{1,0\,j} x) + Y_{20} q_{1,0\,j} H_k(q_{2,0\,j} x) \right) +
$$

$$
+ \sum_{n=1}^{\infty} \sum_{l=1}^{3} X_{ln} \left(k_2 p_{l,nk} - k^* \alpha_{nk} B_{l,nk} \right) H_j(p_{l,nk} y) T_k(\alpha_{nk} x) + \sum_{n=1}^{\infty} \sum_{l=1}^{3} Y_{ln} \left(k^* q_{l,nj} - k_2 \beta_{nj} G_{l,nj} \right) H_k(q_{l,nj} x) T_j(\beta_{nj} y); \qquad (47)
$$

$$
-\frac{M_{xy,kj}}{D_{11}} = k_6 \sum_{n=1}^{\infty} \sum_{l=1}^{3} X_{ln} \left(\alpha_{nk} + p_{l,nk} B_{l,nk} \right) H_j'(p_{l,nk} y) T_k'(\alpha_{nk} x) + k_6 \sum_{n=1}^{\infty} \sum_{l=1}^{3} Y_{ln} \left(\beta_{nj} + q_{l,nj} G_{l,nj} \right) H_k'(q_{l,nj} x) T_j'(\beta_{nj} y); \qquad (48)
$$

$$
\frac{Q_{x,kj}}{D_{11}} = k_4 \delta_{j0} \left(Y_{10} \left(q_{1,0\,j} E_{1,0\,j} - 1 \right) H_k'(q_{1,0\,j} x) + Y_{20} \left(q_{2,0\,j} E_{2,0\,j} - 1 \right) H_k'(q_{2,0\,j} x) \right) +
$$

$$
+ k_4 \sum_{n=1}^{\infty} \sum_{l=1}^{3} X_{ln} \left(\alpha_{nk} A_{l,nk} - B_{l,nk} \right) H_j(p_{l,nk} y) T_k'(\alpha_{nk} x) + k_4 \sum_{n=1}^{\infty} \sum_{l=1}^{3} Y_{ln} \left(q_{l,nj} E_{l,nj} - 1 \right) H_k'(q_{l,nj} x) T_j(\beta_{nj} y); \qquad (49)
$$

$$\frac{Q_{y,kj}}{D_{11}} = k_5\delta_{k0}\left(X_{10}\left(p_{1,0k}A_{1,0k}-1\right)H_j'(p_{1,0k}y)+X_{20}\left(p_{2,0k}A_{2,0k}-1\right)H_j'(p_{2,0k}y)\right)+$$

$$+k_5\sum_{n=1}^{\infty}\sum_{l=1}^{3}X_{ln}\left(p_{l,nk}A_{l,nk}-1\right)H_j'(p_{l,nk}y)T_k(\alpha_{nk}x)+k_5\sum_{n=1}^{\infty}\sum_{l=1}^{3}Y_{ln}\left(\beta_{nj}E_{l,nj}-G_{l,nj}\right)H_k(q_{l,nj}x)T_j'(\beta_{nj}y)\,. \quad (50)$$

where $k^* = \tilde{k} - k_6$.

The next step is to express the unknowns coefficients X_{ln} and Y_{ln} for each type of symmetry (k, j) by means of Fourier coefficients boundary values of Eqs. (45). It should be noted, that the series of the general solution for $\phi_{y,kj}$, $\frac{Q_{x,kj}}{D_{11}}$ and $\frac{M_{xy,kj}}{D_{11}}$ given by Eqs. (43), (48), (49), respectively, can be represented at the boundaries $x = \pm a$ in the form of complete Fourier series due to the equality condition $T_k'(\alpha_{nk}a) = 0$, as follows

$$\phi_{y,kj} = \delta_{j0}\left(Y_{10}H_k'(q_{1,0j}a)+Y_{20}H_k'(q_{2,0j}a)\right)+\sum_{n=1}^{\infty}\sum_{l=1}^{3}Y_{ln}H_k'(q_{l,nj}a)T_j(\beta_{nj}y)=\phi_{y0}^{a,kj}+\sum_{n=1}^{\infty}\phi_{yn}^{a,kj}T_j(\beta_{nj}y) \quad (51)$$

$$\frac{Q_{x,kj}}{D_{11}} = k_4\delta_{j0}\left(Y_{10}\left(q_{1,0j}E_{1,0j}-1\right)H_k'(q_{1,0j}a)+Y_{20}\left(q_{2,0j}E_{2,0j}-1\right)H_k'(q_{2,0j}a)\right)+$$

$$+k_4\sum_{n=1}^{\infty}\sum_{l=1}^{3}Y_{ln}\left(q_{l,nj}E_{l,nj}-1\right)H_k'(q_{l,nj}a)T_j(\beta_{nj}y)=Q_{x0}^{a,kj}+\sum_{n=1}^{\infty}Q_{xn}^{a,kj}T_j(\beta_{nj}y) \quad (52)$$

$$-\frac{M_{xy,kj}}{D_{11}} = k_6\sum_{n=1}^{\infty}\sum_{l=1}^{3}Y_{ln}\left(\beta_{nj}+q_{l,nj}G_{l,nj}\right)H_k'(q_{l,nj}a)T_j'(\beta_{nj}y)=\sum_{n=1}^{\infty}M_{xyn}^{a,kj}T_j'(\beta_{nj}y) \quad (53)$$

where

$$\phi_{yn}^{a,kj} = \frac{\phi_{yn}^{+a,j}-(-1)^k\phi_{yn}^{-a,j}}{2};\ Q_{xn}^{a,kj} = \frac{Q_{xn}^{+a,j}-(-1)^kQ_{xn}^{-a,j}}{2};\ M_{xyn}^{a,kj} = \frac{M_{xyn}^{+a,j}-(-1)^kM_{xyn}^{-a,j}}{2}. \quad (54)$$

Equality of coefficients by basic functions in Eqs. (51) – (53) enables one to determine the unknown coefficients Y_{ln} as follows

$$Y_{10}H_k'(q_{1,0j}a) = \frac{k_4q_{1,0j}^2+\Omega^4}{k_4^2\Omega^4\left(q_{1,0j}^2-q_{2,0j}^2\right)}\left(Q_{x0}^{a,kj}\left(k_4q_{2,0j}^2+\Omega^4\right)+\phi_{y0}^{a,kj}k_4\Omega^4\right) \quad (55)$$

$$Y_{20}H_k'(q_{2,0j}a) = -\frac{k_4q_{2,0j}^2+\Omega^4}{k_4^2\Omega^4\left(q_{1,0j}^2-q_{2,0j}^2\right)}\left(Q_{x0}^{a,kj}\left(k_4q_{1,0j}^2+\Omega^4\right)+\phi_{y0}^{a,kj}k_4\Omega^4\right) \quad (56)$$

and

$$\mathbf{T}_n\begin{pmatrix}Y_{1n}H_k'(q_{1,nj}a)\\ Y_{2n}H_k'(q_{2,nj}a)\\ Y_{3n}H_k'(q_{3,nj}a)\end{pmatrix} = \begin{pmatrix}\phi_{yn}^{a,kj}\\ Q_{xn}^{a,kj}/k_4\\ M_{xyn}^{a,kj}/k_6\end{pmatrix}, \quad (57)$$

where T_n is given by

$$\mathrm{T}_n = \begin{pmatrix} 1 & 1 & 1 \\ q_{1,nj}E_{1,nj} - 1 & q_{2,nj}E_{2,nj} - 1 & q_{3,nj}E_{3,nj} - 1 \\ \beta_{nj} + q_{1,nj}G_{1,nj} & \beta_{nj} + q_{2,nj}G_{2,nj} & \beta_{nj} + q_{3,nj}G_{3,nj} \end{pmatrix} \tag{58}$$

Denoting cofactors to the elements of matrix by $(\mathrm{T}_n)_{sl}$ as $\widetilde{\mathrm{T}}_{nsl}$, respectively, we can write

$$Y_{ln}H'_k(q_{l,nj}a) = \frac{1}{\det \mathrm{T}_n}\left(\widetilde{\mathrm{T}}_{n1l}\phi_{yn}^{a,kj} + \frac{1}{k_4}\widetilde{\mathrm{T}}_{n2l}Q_{xn}^{a,kj} + \frac{1}{k_6}\widetilde{\mathrm{T}}_{n3l}M_{xyn}^{a,kj}\right) \tag{59}$$

In the same manner noting that $T'_j(\beta_{nj}b) = 0$ the series of the general solution for $\phi_{x,kj}$, $\dfrac{Q_{y,kj}}{D_{11}}$ and $\dfrac{M_{xy,kj}}{D_{11}}$ of Eqs. (44), (48), (50) are represented at the boundaries $y = \pm b$ in the form of complete Fourier series as follows

$$\phi_{x,kj} = \delta_{k0}\left(X_{10}H'_j(p_{1,0k}b) + X_{20}H'_j(p_{2,0k}b)\right) + \sum_{n=1}^{\infty}\sum_{l=1}^{3} X_{ln}H'_j(p_{l,nk}b)T_k(\alpha_{nk}x) = \phi_{x0}^{b,kj} + \sum_{n=1}^{\infty}\phi_{xn}^{b,kj}T_k(\alpha_{nk}x); \tag{60}$$

$$\frac{Q_{y,kj}}{D_{11}} = k_5\delta_{k0}\left(X_{10}\left(p_{1,0k}A_{1,0k} - 1\right)H'_j(p_{1,0k}b) + X_{20}\left(p_{2,0k}A_{2,0k} - 1\right)H'_j(p_{2,0k}b)\right) +$$

$$+ k_5\sum_{n=1}^{\infty}\sum_{l=1}^{3} X_{ln}\left(p_{l,nk}A_{l,nk} - 1\right)H'_j(p_{l,nk}b)T_k(\alpha_{nk}x) = Q_{y0}^{b,kj} + \sum_{n=1}^{\infty}Q_{yn}^{b,kj}T_k(\alpha_{nk}x); \tag{61}$$

$$-\frac{M_{xy,kj}}{D_{11}} = k_6\sum_{n=1}^{\infty}\sum_{l=1}^{3} X_{ln}\left(\alpha_{nk} + p_{l,nk}B_{l,nk}\right)H'_j(p_{l,nk}b)T'_k(\alpha_{nk}x) = \sum_{n=1}^{\infty}M_{xyn}^{b,kj}T'_k(\alpha_{nk}x) \tag{62}$$

where

$$\phi_{xn}^{b,kj} = \frac{\phi_{xn}^{+b,k} - (-1)^j\phi_{xn}^{-a,k}}{2};\ Q_{yn}^{b,kj} = \frac{Q_{yn}^{+b,k} - (-1)^j Q_{yn}^{-b,j}}{2};\ M_{xyn}^{b,kj} = \frac{M_{xyn}^{+b,k} - (-1)^j M_{xyn}^{-b,k}}{2} \tag{63}$$

Then the values of unknowns X_{ln} can be found from Eqs. (60)- (62) as

$$X_{10}H'_j(p_{1,0k}b) = \frac{k_5p_{1,0k}^2 + \Omega^4}{k_5^2\Omega^4\left(p_{1,0k}^2 - p_{2,0k}^2\right)}\left(Q_{y0}^{b,kj}\left(k_5p_{2,0k}^2 + \Omega^4\right) + \phi_{x0}^{b,kj}k_5\Omega^4\right) \tag{64}$$

$$X_{20}H'_j(p_{2,0k}b) = -\frac{k_5p_{2,0k}^2 + \Omega^4}{k_5^2\Omega^4\left(p_{1,0k}^2 - p_{2,0k}^2\right)}\left(Q_{y0}^{b,kj}\left(k_5p_{1,0k}^2 + \Omega^4\right) + \phi_{x0}^{b,kj}k_5\Omega^4\right) \tag{65}$$

and

$$X_{ln}H'_j(p_{l,nk}b) = \frac{1}{\det S_n}\left(\widetilde{\mathrm{S}}_{n1l}\phi_{xn}^{b,kj} + \frac{1}{k_5}\widetilde{\mathrm{S}}_{n2l}Q_{yn}^{b,kj} + \frac{1}{k_6}\widetilde{\mathrm{S}}_{n3l}M_{xyn}^{b,kj}\right) \tag{66}$$

where $\widetilde{S}_{nsl}$ denotes the cofactors of the corresponding elements of the S_n matrix given below

$$S_n = \begin{pmatrix} 1 & 1 & 1 \\ p_{1,nk}A_{1,nk} - 1 & p_{2,nk}A_{2,nk} - 1 & p_{3,nk}A_{3,nk} - 1 \\ \alpha_{nk} + p_{1,nk}B_{1,nk} & \alpha_{nk} + p_{2,nk}B_{2,nk} & \alpha_{nk} + p_{3,nk}B_{3,nk} \end{pmatrix} \tag{67}$$

Thus, Eqs. (55), (56), (59), (64) - (66) allow the elimination of all unknowns coefficients X_{ln} and Y_{ln} for each type of symmetry (*k*, *j*) from the general solution and then express the components of displacement and force vectors by means of $\phi_{yn}^{a,kj}$, $Q_{xn}^{a,kj}$, $M_{xyn}^{a,kj}$, $\phi_{xn}^{b,kj}$, $Q_{yn}^{b,kj}$, $M_{xyn}^{b,kj}$ which are connected to Fourier coefficients of Eqs. (45).

In order to construct the dynamic stiffness matrix, it is now necessary to consider the boundary values of $W^{\pm a}$, $\phi_x^{\pm a}$, $M_x^{\pm a}$, $W^{\pm b}$, $\phi_y^{\pm b}$ and $M_y^{\pm b}$. Therefore, by substituting Eqs. (42)-(44), (46) and (47) into the prescribed boundary expansions of Eqs. (45) and introducing Fourier coefficients $W_m^{\pm a,j}$, $\phi_{xm}^{\pm a,j}$, $M_{xm}^{\pm a,j}$, $W_m^{\pm b,k}$, $\phi_{ym}^{\pm b,k}$ and $M_{ym}^{\pm b,k}$ for their symmetrical and anti-symmetrical combinations, one obtains

$$W_m^{a,kj} = \frac{W_m^{+a,j} + (-1)^k W_m^{-a,j}}{2},\ W_m^{b,kj} = \frac{W_m^{+b,k} + (-1)^j W_m^{-b,k}}{2} \quad \text{etc.} \tag{68}$$

Equation (68) gives six functional equations as shown below.

$$W_{kj}(a,y) = \delta_{k0}\left(X_{10}A_{1,0k}H_j(p_{1,0k}y) + X_{20}A_{2,0k}H_j(p_{2,0k}y)\right) + \delta_{j0}\left(Y_{10}E_{1,0j}H_k(q_{1,0j}a) + Y_{20}E_{2,0j}H_k(q_{2,0j}a)\right) +$$
$$+ \sum_{n=1}^{\infty}\sum_{l=1}^{3}(-1)^{n+k}X_{ln}A_{l,nk}H_j(p_{l,nk}y) + \sum_{n=1}^{\infty}\sum_{l=1}^{3}Y_{ln}E_{l,nj}H_k(q_{l,nj}a)T_j(\beta_{nj}y) = \delta_{j0}W_0^{a,k0} + \sum_{n=1}^{\infty}W_n^{a,kj}T_j(\beta_{nj}y); \tag{69}$$

$$W_{kj}(x,b) = \delta_{k0}\left(X_{10}A_{1,0k}H_j(p_{1,0k}b) + X_{20}A_{2,0k}H_j(p_{2,0k}b)\right) + \delta_{j0}\left(Y_{10}E_{1,0j}H_k(q_{1,0j}x) + Y_{20}E_{2,0j}H_k(q_{2,0j}x)\right) +$$
$$+ \sum_{n=1}^{\infty}\sum_{l=1}^{3}X_{ln}A_{l,nk}H_j(p_{l,nk}b)T_k(\alpha_{nk}x) + \sum_{n=1}^{\infty}\sum_{l=1}^{3}(-1)^{n+j}Y_{ln}E_{l,nj}H_k(q_{l,nj}x) = \delta_{k0}W_0^{b,0j} + \sum_{n=1}^{\infty}W_n^{b,kj}T_k(\alpha_{nk}x); \tag{70}$$

$$\phi_{x,kj}(a,y) = \delta_{k0}\left(X_{10}H_j'(p_{1,0k}y) + X_{20}H_j'(p_{2,0k}y)\right) + \sum_{n=1}^{\infty}\sum_{l=1}^{3}(-1)^{n+k}X_{ln}H_j'(p_{l,nk}y) +$$
$$+ \sum_{n=1}^{\infty}\sum_{l=1}^{3}Y_{ln}G_{l,nj}H_k(q_{l,nj}a)T_j'(\beta_{nj}y) = \sum_{n=1}^{\infty}\phi_{xn}^{a,kj}T_j'(\beta_{nj}y); \tag{71}$$

$$\phi_{y,kj}(x,b) = \delta_{j0}\left(Y_{10}H_k'(q_{1,0j}x) + Y_{20}H_k'(q_{2,0j}x)\right) + \sum_{n=1}^{\infty}\sum_{l=1}^{3}X_{ln}B_{l,nk}H_j(p_{l,nk}b)T_k'(\alpha_{nk}x) +$$
$$+ \sum_{n=1}^{\infty}\sum_{l=1}^{3}(-1)^{n+j}Y_{ln}H_k'(q_{l,nj}x) = \sum_{n=1}^{\infty}\phi_{yn}^{b,kj}T_k'(\alpha_{nk}x); \tag{72}$$

$$-\frac{M_{x,kj}(a,y)}{D_{11}} = k^*\delta_{k0}\left(X_{10}p_{1,0k}H_j(p_{1,0k}y)+X_{20}p_{2,0k}H_j(p_{2,0k}y)\right)+\delta_{j0}\left(Y_{10}q_{1,0\,j}H_k(q_{1,0\,j}a)+Y_{20}q_{1,0\,j}H_k(q_{2,0\,j}a)\right)+$$

$$+\sum_{n=1}^{\infty}\sum_{l=1}^{3}(-1)^{n+k}X_{ln}\left(k^*p_{l,nk}-\alpha_{nk}B_{l,nk}\right)H_j(p_{l,nk}y)+\sum_{n=1}^{\infty}\sum_{l=1}^{3}Y_{ln}\left(q_{l,nj}-k^*\beta_{nj}G_{l,nj}\right)H_k(q_{l,nj}a)T_j(\beta_{nj}y)=$$

$$=\delta_{j0}M_{x0}^{a,k0}+\sum_{n=1}^{\infty}M_{xn}^{a,kj}T_j(\beta_{nj}y); \tag{73}$$

$$-\frac{M_{y,kj}(x,b)}{D_{11}} = k_2\delta_{k0}\left(X_{10}p_{1,0k}H_j(p_{1,0k}b)+X_{20}p_{2,0k}H_j(p_{2,0k}b)\right)+\delta_{j0}k^*\left(Y_{10}q_{1,0\,j}H_k(q_{1,0\,j}x)+Y_{20}q_{1,0\,j}H_k(q_{2,0\,j}x)\right)+$$

$$+\sum_{n=1}^{\infty}\sum_{l=1}^{3}X_{ln}\left(k_2p_{l,nk}-k^*\alpha_{nk}B_{l,nk}\right)H_j(p_{l,nk}b)T_k(\alpha_{nk}x)+\sum_{n=1}^{\infty}\sum_{l=1}^{3}(-1)^{n+j}Y_{ln}\left(k^*q_{l,nj}-k_2\beta_{nj}G_{l,nj}\right)H_k(q_{l,nj}x)=$$

$$=\delta_{k0}M_{y0}^{b,0\,j}+\sum_{n=1}^{\infty}M_{yn}^{b,kj}T_k(\alpha_{nk}x) \tag{74}$$

It is to be noted that for any component case of the symmetry due to the similarity of expansion into Fourier series of $\cosh t$ with respect to the system $\cos\frac{\pi n\mathrm{t}}{T}$ and expansion of $\sinh t$ with respect to the system $\sin\frac{\pi(2n-1)t}{2T}$ when $t\in[-T;T]$, one can obtain the following Fourier expansions

$$\frac{H_k(qx)}{H_k'(qa)} = \frac{\delta_{k0}}{aq}+\frac{2q}{a}\sum_{m=1}^{\infty}\frac{(-1)^{m+k}T_k(\alpha_{mk}x)}{\alpha_{mk}^2+q^2} \tag{75}$$

$$\frac{H_k'(qx)}{H_k'(qa)} = \frac{2}{a}\sum_{m=1}^{\infty}\frac{(-1)^{m+k}\alpha_{mk}T_k'(\alpha_{mk}x)}{\alpha_{mk}^2+q^2} \tag{76}$$

$$\frac{H_j(py)}{H_j'(pb)} = \frac{\delta_{j0}}{bp}+\frac{2p}{b}\sum_{m=1}^{\infty}\frac{(-1)^{m+j}T_j(\beta_{mj}y)}{\beta_{mj}^2+p^2} \tag{77}$$

$$\frac{H_j'(py)}{H_j'(pb)} = \frac{2}{b}\sum_{m=1}^{\infty}\frac{(-1)^{m+j}\beta_{mj}T_j'(\beta_{mj}y)}{\beta_{mj}^2+p^2} \tag{78}$$

Substituting the Eqs. (75) - (78) in the Eqs. (69) - (74) and changing the order of summation for the double series, one can rewrite Eqs. (69) - (74) in the form of complete Fourier series. With this scheme and by making the following substitutions

$$x_{ln} = X_{ln}H_j'(p_{l,nk}b),\ y_{ln} = Y_{ln}H_k'(q_{l,nj}a) \tag{79}$$

and introducing the following notation for brevity

$$\mathrm{Th}_k(z) = \frac{H_k(z)}{H_k'(z)} \tag{80}$$

the equalities for constant terms eventually lead to the following equations

$$\frac{\delta_{k0}\delta_{j0}}{b}\left(\frac{A_{1,0k}x_{10}}{p_{1,0k}}+\frac{A_{2,0k}x_{20}}{p_{2,0k}}\right)+\delta_{j0}\left(E_{1,0\,j}\mathrm{Th}_k(q_{1,0\,j}a)y_{10}+E_{2,0\,j}\mathrm{Th}_k(q_{2,0\,j}a)y_{20}\right)+$$

$$+\delta_{j0}\sum_{n=1}^{\infty}\sum_{l=1}^{3}\frac{(-1)^{n+k}A_{l,nk}}{bp_{l,nk}}x_{ln}=\delta_{j0}W_0^{a,k0} \tag{81}$$

$$\delta_{k0}\left(A_{1,0k}\mathrm{Th}_j(p_{1,0k}b)x_{10}+A_{2,0k}\mathrm{Th}_j(p_{2,0k}b)x_{20}\right)+\frac{\delta_{k0}\delta_{j0}}{a}\left(\frac{E_{1,0\,j}y_{10}}{q_{1,0\,j}}+\frac{E_{2,0\,j}y_{20}}{q_{2,0\,j}}\right)+$$

$$+\delta_{k0}\sum_{n=1}^{\infty}\sum_{l=1}^{3}\frac{(-1)^{n+j}E_{l,nj}}{aq_{l,nj}}y_{ln}=\delta_{k0}W_0^{b,0\,j} \tag{82}$$

$$\frac{\delta_{k0}\delta_{j0}k^*}{b}(x_{10}+x_{20})+\delta_{j0}\left(q_{1,0\,j}\mathrm{Th}_k(q_{1,0\,j}a)y_{10}+q_{2,0\,j}\mathrm{Th}_k(q_{2,0\,j}a)y_{20}\right)+$$

$$+\delta_{j0}\sum_{n=1}^{\infty}\sum_{l=1}^{3}\frac{(-1)^{n+k}}{bp_{l,nk}}\left(k^*p_{l,nk}-\alpha_{nk}B_{l,nk}\right)x_{ln}=\delta_{j0}M_{x0}^{a,k0} \tag{83}$$

$$\delta_{k0}k_2\left(p_{1,0k}\mathrm{Th}_j(p_{1,0k}b)x_{10}+p_{2,0k}\mathrm{Th}_j(p_{2,0k}b)x_{20}\right)+\frac{\delta_{k0}\delta_{j0}k^*}{a}(y_{10}+y_{20})+$$

$$+\delta_{k0}\sum_{n=1}^{\infty}\sum_{l=1}^{3}\frac{(-1)^{n+j}}{aq_{l,nj}}\left(k^*q_{l,nj}-k_2\beta_{nj}G_{l,nj}\right)y_{ln}=\delta_{k0}M_{y0}^{b,0\,j} \tag{84}$$

An equality of Fourier coefficients for basic functions $T_k(\alpha_{mk}x)$ and $T_j(\beta_{mj}y)$ makes it possible to write the rest part of the equations of the infinite system in the following algebraic forms

$$\frac{2\delta_{k0}}{b}\left(\frac{A_{1,0k}p_{1,0k}x_{10}}{\beta_{mj}^2+p_{1,0k}^2}+\frac{A_{2,0k}p_{2,0k}x_{20}}{\beta_{mj}^2+p_{2,0k}^2}\right)+\frac{2}{b}\sum_{n=1}^{\infty}\sum_{l=1}^{3}\frac{(-1)^{n+k}A_{l,nk}p_{l,nk}x_{ln}}{\beta_{mj}^2+p_{l,nk}^2}+$$

$$+(-1)^{m+j}\sum_{l=1}^{3}E_{l,mj}\mathrm{Th}_k(q_{l,mj}a)y_{lm}=(-1)^{m+j}W_m^{a,kj} \tag{85}$$

$$\frac{2\delta_{j0}}{a}\left(\frac{E_{1,0\,j}q_{1,0\,j}y_{10}}{\alpha_{mk}^2+q_{1,0\,j}^2}+\frac{E_{2,0\,j}q_{2,0\,j}y_{20}}{\alpha_{mk}^2+q_{2,0\,j}^2}\right)+\frac{2}{a}\sum_{n=1}^{\infty}\sum_{l=1}^{3}\frac{(-1)^{n+j}E_{l,nj}q_{l,nj}y_{ln}}{\alpha_{mk}^2+q_{l,nj}^2}+$$

$$+(-1)^{m+k}\sum_{l=1}^{3}A_{l,mk}\mathrm{Th}_j(p_{l,mk}b)x_{lm}=(-1)^{m+k}W_m^{b,kj} \tag{86}$$

$$\frac{2\delta_{k0}}{b}\left(\frac{x_{10}}{\beta_{mj}^2+p_{1,0k}^2}+\frac{x_{20}}{\beta_{mj}^2+p_{2,0k}^2}\right)+\frac{2}{b}\sum_{n=1}^{\infty}\sum_{l=1}^{3}\frac{(-1)^{n+k}x_{ln}}{\beta_{mj}^2+p_{l,nk}^2}+\frac{(-1)^{m+j}}{\beta_{mj}}\sum_{l=1}^{3}G_{l,mj}\mathrm{Th}_k(q_{l,mj}a)y_{lm}=$$

$$=\frac{(-1)^{m+j}\phi_{xm}^{a,kj}}{\beta_{mj}} \tag{87}$$

$$\frac{2\delta_{j0}}{a}\left(\frac{y_{10}}{\alpha_{mk}^2+q_{1,0\,j}^2}+\frac{y_{20}}{\alpha_{mk}^2+q_{2,0\,j}^2}\right)+\frac{2}{a}\sum_{n=1}^{\infty}\sum_{l=1}^{3}\frac{(-1)^{n+j}y_{ln}}{\alpha_{mk}^2+q_{l,nj}^2}+\frac{(-1)^{m+k}}{\alpha_{mk}}\sum_{l=1}^{3}B_{l,mk}\mathrm{Th}_{\,j}(p_{l,mk}b)x_{lm}=$$

$$=\frac{(-1)^{m+k}\phi_{ym}^{b,kj}}{\alpha_{mk}} \tag{88}$$

$$\frac{2\delta_{k0}k^*}{b}\left(\frac{p_{1,0k}^2x_{10}}{\beta_{mj}^2+p_{1,0k}^2}+\frac{p_{2,0k}^2x_{20}}{\beta_{mj}^2+p_{2,0k}^2}\right)+\frac{2}{b}\sum_{n=1}^{\infty}\sum_{l=1}^{3}\frac{(-1)^{n+k}p_{l,nk}}{\beta_{mj}^2+p_{l,nk}^2}\left(k^*p_{l,nk}-\alpha_{nk}B_{l,nk}\right)x_{ln}+$$

$$+(-1)^{m+j}\sum_{l=1}^{3}\left(q_{l,mj}-k^*\beta_{mj}G_{l,mj}\right)\mathrm{Th}_{\,k}(q_{l,mj}a)y_{lm}=(-1)^{m+j}M_{xm}^{a,kj} \tag{89}$$

$$\frac{2\delta_{j0}k^*}{a}\left(\frac{q_{1,0\,j}^2y_{10}}{\alpha_{mk}^2+q_{1,0\,j}^2}+\frac{q_{2,0\,j}^2y_{20}}{\alpha_{mk}^2+q_{2,0\,j}^2}\right)+\frac{2}{a}\sum_{n=1}^{\infty}\sum_{l=1}^{3}\frac{(-1)^{n+j}q_{l,nj}}{\alpha_{mk}^2+q_{l,nj}^2}\left(k^*q_{l,nj}-k_2\beta_{nj}G_{l,nj}\right)y_{ln}+$$

$$+(-1)^{m+k}\sum_{l=1}^{3}\left(k_2p_{l,mk}-k^*\alpha_{mk}B_{l,mk}\right)\mathrm{Th}_{\,j}(p_{l,mk}b)x_{lm}=(-1)^{m+k}M_{ym}^{b,kj} \tag{90}$$

$$(m=1,\,2,\,\ldots.\infty)$$

The infinite system of linear equations of Eqs. (81) – (90) connects all Fourier coefficients at the boundaries, see Eq. (45) together with the Eqs. (55), (56), (59), (64) - (66). Basically, the infinite system derived above defines the dynamic stiffness matrix for an orthotropic Mindlin plate entirely. (It should be noted, that development of the dynamic stiffness matrix can be greatly facilitated with help of matrix algebra, i.e. symbolic computation.) Introducing the following sub-vectors of Fourier coefficients

$$\tilde{d}^{\pm a}=\left[W_0^{\pm a},\phi_{y0}^{\pm a},\phi_{x0}^{\pm a},W_1^{\pm a,1},\phi_{y1}^{\pm a,1},\phi_{x1}^{\pm a,1},W_m^{\pm a,0},\phi_{y1}^{\pm a,0},\phi_{x1}^{\pm a,0},\ldots,W_m^{\pm a,1},\phi_{ym}^{\pm a,1},\phi_{xm}^{\pm a,1},W_m^{\pm a,0},\phi_{ym}^{\pm a,0},\phi_{xm}^{\pm a,0},\ldots\right]^T; \tag{91}$$

$$\tilde{d}^{\pm b}=\left[W_0^{\pm b},\phi_{y0}^{\pm b},\phi_{x0}^{\pm b},W_1^{\pm b,1},\phi_{y1}^{\pm b,1},\phi_{x1}^{\pm b,1},W_m^{\pm b,0},\phi_{y1}^{\pm b,0},\phi_{x1}^{\pm b,0},\ldots,W_m^{\pm b,1},\phi_{ym}^{\pm b,1},\phi_{xm}^{\pm b,1},W_m^{\pm b,0},\phi_{ym}^{\pm b,0},\phi_{xm}^{\pm b,0},\ldots\right]^T; \tag{92}$$

$$\tilde{f}^{\pm a}=\left[M_{x0}^{\pm a},Q_{x0}^{\pm a},M_{xy0}^{\pm a},M_{x1}^{\pm a,1},Q_{x1}^{\pm a,1},M_{xy1}^{\pm a,1},M_{x1}^{\pm a,0},Q_{x1}^{\pm a,0},M_{xy1}^{\pm a,0},\ldots,M_{xm}^{\pm a,1},Q_{xm}^{\pm a,1},M_{xym}^{\pm a,1},M_{xm}^{\pm a,0},Q_{xm}^{\pm a,0},M_{xym}^{\pm a,0},\ldots\right]^T \tag{93}$$

$$\tilde{f}^{\pm b}=\left[M_{y0}^{\pm b},Q_{y0}^{\pm b},M_{xy0}^{\pm b},M_{y1}^{\pm b,1},Q_{y1}^{\pm b,1},M_{xy1}^{\pm b,1},M_{y1}^{\pm b,0},Q_{y1}^{\pm b,0},M_{xy1}^{\pm b,0},\ldots,M_{ym}^{\pm b,1},Q_{ym}^{\pm b,1},M_{xym}^{\pm b,1},M_{ym}^{\pm b,0},Q_{ym}^{\pm b,0},M_{xym}^{\pm b,0},\ldots\right]^T \tag{94}$$

where the superscript (upper suffix) *T* denotes a transpose.

The infinite system described above can now be written in matrix form as follows

$$\mathrm{K}_f\,\tilde{f}=\mathrm{K}_d\tilde{d} \tag{95}$$

where

$$\tilde{f}=\left[\tilde{f}^{+a},\tilde{f}^{+b},\tilde{f}^{-a},\tilde{f}^{-b}\right]^T;\tilde{d}=\left[\tilde{d}^{+a},\tilde{d}^{+b},\tilde{d}^{-a},\tilde{d}^{-b}\right]^T \tag{96}$$

It should be noted that for all sequences of Fourier coefficients, each of the expressions presented above, is exact in the sense that it can be computed up to any desired accuracy or to be precise up to machine accuracy if needed. However, for practical applications these sequences and the equations of infinite system of Eqs (81) – (90) need to be truncated at some stage. One of the most traditional ways of solving an infinite system called the "method of reduction" is used in the subsequent text.

Finally, by truncating Eq. (95) by some number, say *N*, for which the coefficients with subscripts higher than the value of *N* can be neglected, it is possible to ascertain the dynamic stiffness matrix in the following form.

$$\tilde{f}_N = \mathrm{K}_N \tilde{d}_N \tag{97}$$

where

$$K_N = (\mathrm{K}_f)^{-1} \mathrm{K}_d \tag{98}$$

is the frequency-dependent dynamic stiffness matrix of the specially orthotropic Mindlin plate.

The above dynamic stiffness matrix K_N can now be used to compute the natural frequencies and mode shapes of either an individual specially orthotropic Mindlin plate, or an assembly of specially orthotropic Mindlin plates for different boundary conditions. A reliable and accurate method of solving the eigenvalue problem is to apply the Wittrick-Williams algorithm [3-6] which is well suited for the DSM applications. The algorithm uses the Sturm sequence property of the dynamic stiffness matrix and ensures that no natural frequencies of the structure analysed are missed. It has featured in hundreds of papers in the literature, but interested readers are referred to the original work of Wittrick and Williams [6] for a detailed insight.

4. Numerical results and discussion

The first set of results was obtained to check the accuracy and the rapidness of convergence of the proposed dynamic stiffness method. To achieve this, the theory is first applied to isotropic Mindlin plates for various boundary conditions. Note that the letters F, C and S are used in sequence when one or more of the plate edges are Free (F), Clamped (C) or Simply Supported (S). The first eight natural frequencies of an isotropic Mindlin plate with free boundary condition at all edges (FFFF) have been computed using the present theory for different values of *N* where *N* is an integer beyond which the Fourier series used in the solution is truncated (See Eq. (97) and the sentence above it). The natural frequencies computed from the proposed DSM are shown in Table 1 in non-dimensional form together with comparative results based on the superposition method taken from the literature [34]. Clearly the natural frequencies obtained from the present theory are close to the ones reported in [34], the greatest discrepancy being around 2%. The difference in the natural frequencies increases with the order of the natural frequency. For most of the natural frequencies reported in Table 1, the accuracy achieved is satisfactory with the value of $N = 4$ and

when N is increased to 8, the natural frequencies convergence very rapidly. Note that the indicator (k, j) where k and j can be either 0 or 1 is included in Table 1 to characterize the nature of the mode. For instance, the first and fifth natural frequencies correspond to the modes which are symmetric about both XZ and YZ planes whereas the third mode is symmetric about XZ plane and anti-symmetric YZ plane and so on and so forth.

Table 1

The first eight natural frequency parameter Ω for a rectangular isotropic Mindlin plate with FFFF boundary conditions for different values of N; $\nu = 0.333, \kappa = 0.8601, h/a = 0.1, b/a = 3$

Method	Natural frequency and mode sequence number							
	1	2	3	4	5	6	7	8
Symmetry (k, j)	(0,0)	(1,1)	(0,1)	(1,0)	(0,0)	(1,1)	(0,1)	(1,0)
DSM $N = 4$	0.7673	1.0252	1.2781	1.4904	1.8021	1.9053	2.2924	2.3195
DSM $N = 8$	0.7670	1.0248	1.2778	1.4902	1.7910	1.9052	2.2825	2.3162
DSM $N = 16$	0.7670	1.0248	1.2776	1.4902	1.7909	1.9046	2.2814	2.3157
Ref. [34]	0.7657	1.0140	1.2715	1.4715	1.7741	1.8748	2.2494	2.2716

It should be noted that the governing differential equations Eq.(5) are satisfied exactly according to the developed approach in the case when the characteristic parameters p and q of Eqs (15) and (28) are defined by the algebraic systems of Eqs. (18) and (33). Program implementation of the theory in the package Mathematica made it possible to solve the system of equation almost exactly for all practical purposes. (Note that an accuracy within the bounds of $\pm 10^{-52}$ can be achieved by using Mathematica.) However, an important criterion for the accuracy in computing the natural frequencies is to ensure the fulfilment of boundary conditions in a satisfactory manner. For the FFFF boundary conditions, two conditions, namely $M_x(a, y) = 0$ and $M_y(x, b) = 0$ are fulfilled when solving the infinite system through series solution whereas other boundary conditions are fulfilled exactly. Table 2 illustrates the degree of accuracy when fulfilling the boundary conditions for the eighth natural frequency given in Table 1. The eighth natural frequency was chosen because it was the highest order natural frequency computed and it showed the biggest difference with published results (see in Table 1). Furthermore, it may be seen from Table 2 that if the value of N is increased, the accuracy of fulfilling the boundary conditions increases although the computed value of the eighth natural frequency is virtually unchanged (see Table 1). In the proposed procedure 16 terms in each series gave excellent agreement to achieve the

prescribed zero distribution of bending moments on the plate edges. However, satisfying the boundary condition at the free edge corner point of the plate is problematic as observed by Papkov [19] and others [38]. The problem is due to the slow convergence of the Fourier series representing the bending moments at the corner of the plate.

Table 2

Convergence test of fulfilling the zero bending moment requirements when computing the eighth natural frequency ($\Omega = 2.3158$) of a rectangular isotropic Mindlin plate free with FFFF boundary conditions; $\nu = 0.333, \kappa = 0.8601, h/a = 0.1, b/a = 3$

$\frac{y}{b}$	$M_x(a,y)/M_{max}$ N =8	$M_x(a,y)/M_{max}$ N =16	$M_x(a,y)/M_{max}$ N =32	$M_x(a,y)/M_{max}$ N =64
0.0	0.0828	0.0138	0.0013	- 0.0001
0.2	- 0.0468	0.0007	- 0.0019	-0.0006
0.4	- 0.0031	- 0.0168	0.0012	-0.0001
0.6	0.0969	- 0.0045	-0.0015	0.0005
0.8	- 0.1719	0.0368	-0.0008	0.0001
1.0	0.2765	- 0.0096	-0.0083	-0.0053
$\frac{x}{a}$	$M_y(x,b)/M_{max}$ N =8	$M_y(x,b)/M_{max}$ N =16	$M_y(x,b)/M_{max}$ N =32	$M_y(x,b)/M_{max}$ N =64
0.0	0.0000	0.0000	0.0000	0.0000
0.2	- 0.0191	0.0003	0.0000	0.0000
0.4	0.0219	0.0005	0.0000	0.0000
0.6	0.0074	- 0.0005	- 0.0001	0.0001
0.8	-0.0482	-0.0036	0.0005	0.0002
1.0	-0.0428	- 0.0122	- 0.0088	-0.0050

The first eight natural frequencies of a square isotropic Mindlin plate using the proposed DSM are shown in Table 3 and Table 4 for CCCC and SFSF boundary conditions, respectively, where the computed natural frequencies are also compared with ones obtained by other researchers using the DSC-element [31] and Rayleigh-Ritz [32] methods. The results shown in Table 3 for the CCCC boundary conditions match very well with published results as can be seen. On the other hand, Table 4 presents results for the relatively easy case of the SFSF boundary conditions which have exact Levy-type solution. However, the current DSM theory does not permit the computation of natural frequencies exactly in a literal sense which is paradoxically an advantage in the present analysis because it provides the opportunity to test the convergence of the results computed from the current theory. Practically the same

type of convergence of results seen in Tables 1 and 3 is observed in Table 4. It can be further noticed from the results in Table 4 that the computed natural frequencies are close to the ones of Ref. [32] when N = 8. In Table 5 the results from the currently developed DSM theory for CFFF boundary condition, i.e. for a cantilever plate, are very close to the published solutions obtained by the DSC-element method [31] and the so called *pb2* Rayleigh-Ritz method [32].

Table 3

The first eight frequency parameters $\tilde{\Omega} = \frac{4\Omega^2}{\pi^2}$ for of a square isotropic Mindlin plate with CCCC boundary conditions for different values of N; $\nu = 0.3, \kappa = 5/6, h/a = 0.1$

Method	Natural frequency and mode sequence number							
	1	2	3	4	5	6	7	8
DSM N = 4	3.3020	6.2967	6.2967	8.8211	10.3842	10.4868	12.5645	12.5645
DSM N = 8	3.3009	6.2929	6.2929	8.8177	10.3801	10.4826	12.5598	2.5598
DSM N = 16	3.3002	6.2926	6.2926	8.8171	10.3793	10.4818	12.5590	12.5590
Ref. [31]	3.2960	6.2873	6.2873	8.8123	10.3791	10.4776	12.5546	12.5546
Ref. [32]	3.2954	6.2858	6.2858	8.8098	10.3788	10.4778	12.5529	12.5529

Table 4

The first eight natural frequency parameters $\tilde{\Omega} = \frac{4\Omega^2}{\pi^2}$ for an isotropic square Mindlin plate with SFSF boundary conditions for different values N; $\nu = 0.3, \kappa = 5/6, h/a = 0.1$

Method	Natural frequency and mode sequence number							
	1	2	3	4	5	6	7	8
DSM N = 4	0.9677	1.5785	3.4503	3.7055	4.3580	6.3194	6.7362	7.7817
DSM N = 8	0.9562	1.5657	3.4387	3.6920	4.3445	6.3067	6.7152	7.7698
DSM N = 16	0.9553	1.5622	3.4355	3.6892	4.3404	6.3019	6.7118	7.7661
Ref. [32]	0.9574	1.5645	3.4328	3.6848	4.3408	6.3006	6.7134	7.7636
Exact results (characteristic equation)	0.9565	1.5593	3.4307	3.6837	4.3358	6.2968	6.7072	7.7645

Table 5

The first eight natural frequency parameters $\tilde{\Omega} = \frac{4\Omega^2}{\pi^2}$ for an isotropic squareMindlin plate with CFFF boundary conditions for $\nu = 0.3, \kappa = 5/6, h/a = 0.1$

Method	Natural frequency and mode sequence number							
	1	2	3	4	5	6	7	8
DSM N = 16	0.3505	0.8170	2.0350	2.5839	2.8621	4.8172	5.4788	5.7741
Ref. [31]	0.3735	0.8403	2.0502	2.5997	2.8752	4.8285	5.4885	5.7860
Ref. [32]	0.3476	0.8168	2.0356	2.5836	2.8620	4.8162	5.4834	57769

Table 6

The first ten natural frequency parameter (Ω_i) for a square glass/epoxy plate with FFFF boundary conditions; $\kappa = 0.8601$ $E_1 = 60.7$ GPa, $G_{12} = G_{13} = G_{23} = 12$ GPa, $\nu_{12} = 0.23$, $\nu_{21} = 0.094$

	Natural frequency and mode sequence number									
	1	2	3	4	5	6	7	8	9	10
CPT	1.5832	1.8792	2.3653	2.4872	2.7349	3.1388	3.4892	3.5140	3.9210	4.1395
$h/a = 0.01$	1.5816	1.8793	2.3652	2.4850	2.7331	3.1386	3.4857	3.5115	3.9201	4.1372
$h/a = 0.05$	1.5747	1.8774	2.3615	2.4721	2.7208	3.1298	3.4601	3.4907	3.9014	4.1105
$h/a = 0.10$	1.5643	1.8716	2.3503	2.4490	2.6963	3.1036	3.4095	3.4451	3.8464	4.0427

Having established the predictable accuracy and rapid convergence of the proposed theory, the first ten natural frequencies for a square orthotropic glass/epoxy Mindlin plate ($b/a = 1$, $\kappa = 0.8601$, $E_1 = 60.7$ GPa, $G_{12} = G_{13} = G_{23} = 12$ GPa, $\nu_{12} = 0.23$, $\nu_{21} = 0.094$) are computed next. These natural frequencies are presented in Table 6 in non-dimensional form for FFFF boundary conditions whereas Table 7 shows results for CCCC boundary conditions whereas Table 8 presents results for CFFF boundary conditions. Three plate thickness ratio (h/a) values of 0.01, 0.05 and 0.1 were chosen when computing the results shown in Tables 6 and 7. For comparison purposes, the values of natural frequencies as calculated by using the dynamic stiffness theory based on classical plate theory (CPT) [18] which does not account for the shear deformation and rotatory inertia are also given in these tables. It should be noted that the natural frequencies calculated in [18] provided close lower and upper bounds for each of the natural frequencies with the help of the criterion of existence for unique solution of infinite

system of linear equations. The lower and upper bounds of the natural frequencies can be made very close to each other so that several digits of accuracy can be achieved. Thus, to all intent and purposes the CPT based results of [18] quoted in Tables 6, 7 can be considered to be exact because the upper bound and lower bounds of the natural frequencies were computed to a very high degree of accuracy. (If needed, these values can be computed even up to machine accuracy.)

Table 7

The first ten natural frequency parameter (Ω_i) for a square glass/epoxy plate with CCCC boundary conditions; $\kappa = 0.8601$ $E_1 = 60.7$ GPa, $G_{12} = G_{13} = G_{23} = 12$ GPa, $\nu_{12} = 0.23$, $\nu_{21} = 0.094$

	Natural frequency and mode sequence number									
	1	2	3	4	5	6	7	8	9	10
CPT	2.6975	3.5649	4.1015	4.6283	4.6678	5.4446	5.6157	5.8497	5.9759	6.4397
$h/a = 0.01$	2.6970	3.5567	4.0999	4.6263	4.6662	5.4372	5.6119	5.8203	5.9681	6.4252
$h/a = 0.05$	2.6858	3.5314	4.0634	4.5802	4.6285	5.3761	5.5280	5.7454	5.8719	6.3410
$h/a = 0.10$	2.6527	3.4575	3.9602	4.4539	4.5223	5.2041	5.3035	5.5521	5.6189	6.0943

Table 8

The first ten natural frequency parameter (Ω_i) for a square glass/epoxy plate with CFFF boundary conditions; $\kappa = 0.8601$ $E_1 = 60.7$ GPa, $G_{12} = G_{13} = G_{23} = 12$ GPa, $\nu_{12} = 0.23$, $\nu_{21} = 0.094$

	Natural frequency and mode sequence number									
	1	2	3	4	5	6	7	8	9	10
$h/a = 0.01$	0.9363	1.3124	2.1443	2.3484	2.6147	3.2433	3.2674	3.9217	4.1035	4.4660
$h/a = 0.05$	0.9357	1.3080	2.1368	2.3417	2.6021	3.2202	3.2540	3.8955	4.0708	4.4362
$h/a = 0.10$	0.9346	1.2998	2.1212	2.3218	2.5725	3.1693	3.2197	3.8198	3.9877	4.3885

Table 6 shows that the values of the FFFF natural frequencies are decreased with increasing values of thickness ratio *h/a* of the plate, as expected. Results for *h/a* = 0.01 when the plate thickness is very small practically coincide with ones obtained from CPT based DSM of [18] because the effects of shear deformation and rotatory inertia are not expected to be great for thin plates. The maximum difference between CPT based results and Mindlin theory results (FSDT) which account for the effects of shear deformation and rotatory inertia is observed to be around 3% when the plate thickness ratio *h/a* = 0.1.

Comparison of the modes shapes for the first, fifth and tenth natural frequencies for *h/a* =0.01 and 0.1 shows that the modes from CPT based DSM and FSDT based DSM for the two cases are very similar with very small quantitative differences, see Fig. 3.

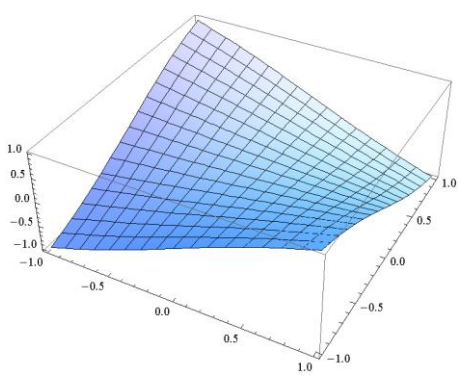

$\Omega_1 = 1.5816,\ h/a = 0.01$

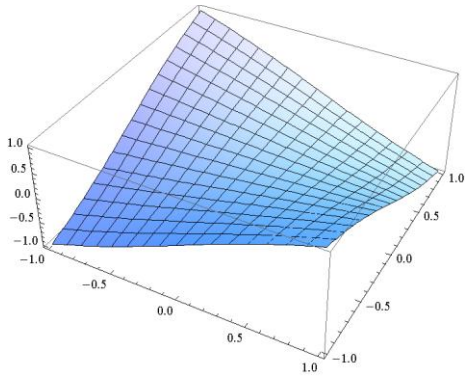

$\Omega_1 = 1.5643,\ h/a = 0.1$

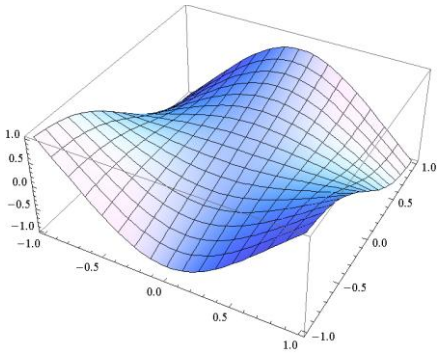

$\Omega_5 = 2.7331,\ h/a = 0.01$

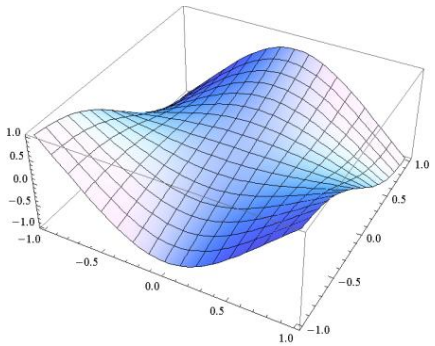

$\Omega_5 = 2.6963,\ h/a = 0.1$

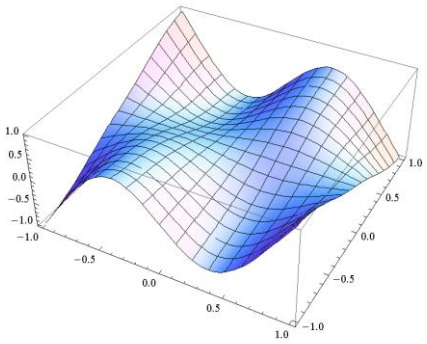

$\Omega_{10} = 4.1372,\ h/a = 0.01$

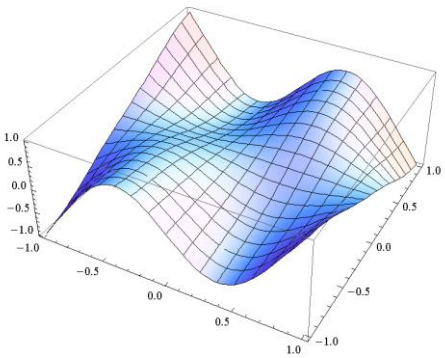

$\Omega_{10} = 4.0427,\ h/a = 0.1$

Fig 3. The 1st, 5th and 10th mode shapes of a square glass/epoxy plate for FFFF boundary conditions

From the results for CCCC boundary conditions shown in Table 7, one can observe a similar trend. Classical plate theory and Mindlin plate theory give close values for natural frequencies when thickness of the plate is small (e.g., *h/a* =0.01). Furthermore, with increasing values of *h/a* the natural

frequencies decrease, as expected. The difference between natural frequencies obtained with the help of CPT and Mindlin (FSDT) dynamic stiffness theories is somehow more pronounced for the CCCC boundary conditions as opposed to the FFFF boundary condition when the maximum discrepancy in results is 5.5%, see Table 7.

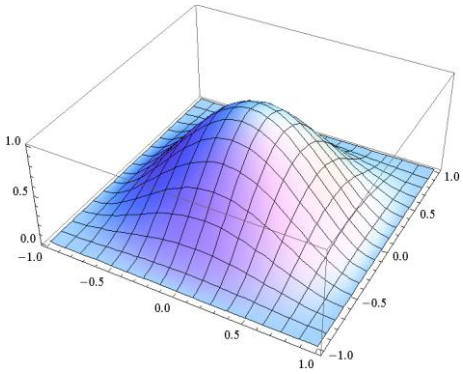

$\Omega_1 = 2.6970,\ h/a = 0.01$

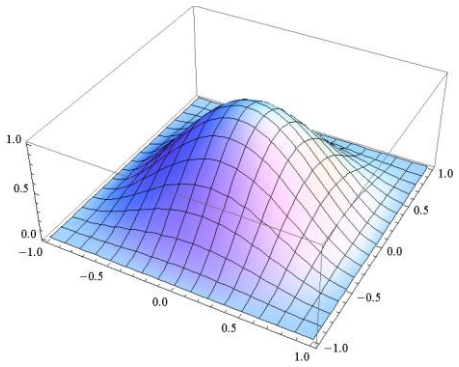

$\Omega_1 = 2.6527,\ h/a = 0.1$

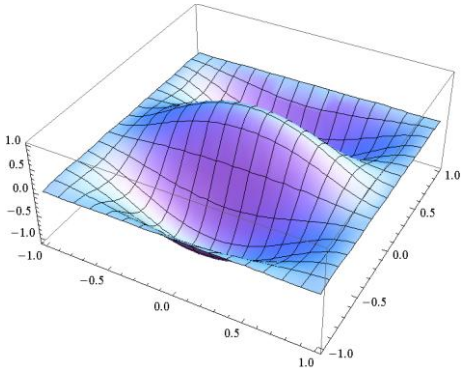

$\Omega_5 = 4.6662,\ h/a = 0.01$

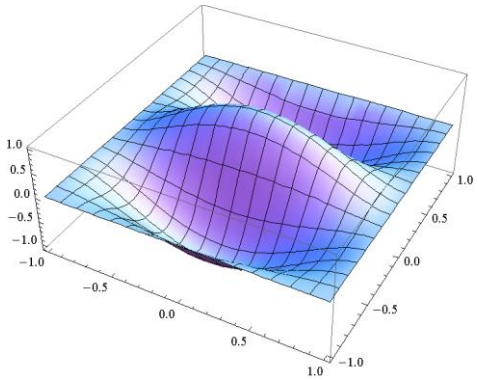

$\Omega_5 = 4.5223,\ h/a = 0.1$

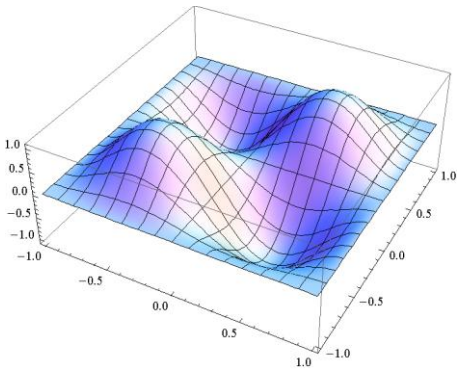

$\Omega_{10} = 6.4252,\ h/a = 0.01$

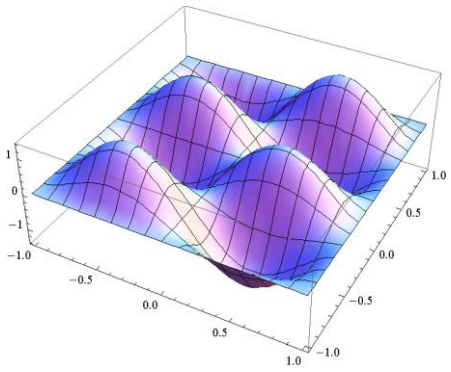

$\Omega_{10} = 6.0943,\ h/a = 0.1$

Fig 4. The 1st, 5th and 10th mode shapes of a square glass/epoxy plate with CCCC boundary conditions

Figure 4 shows the mode shapes for CCCC boundary conditions of the specially othotropic Mindlin plate. There are only little quantitative differences in the mode shapes, particularly for the lower order

modes. Nevertheless, with increasing sequence number of the mode shapes, one can observe bigger differences, see Fig. 4. For instance, the 10th mode shows an appreciable difference between the CPT based DSM and Mindlin (FSDT) based DSM mode shapes.

5. Future potential and practical applications of the theory

The above dynamic stiffness theory is of great significance with potential possibilities in computer aided structural analysis and design. One of the great advantages of the proposed method is its uncompromising accuracy together with its computational efficiency, particularly when carrying out modal analysis in the high frequency range for which the conventional finite element method can become inaccurate or even unreliable. Moreover, the estimation of flow of vibrational energy in structures is a subject of considerable importance, particularly when using the statistical energy analysis method [1, 2] for which the modal density in the high frequency range is an essential prerequisite. It is well known that the traditional finite element method is deficient in this respect. By contrast, the proposed method based on rigorous mathematical theory of elasticity is exact in that the results can be computed up to any desired accuracy with no approximations made en route. It is thus ideally suited for modal analysis in all frequency ranges. The application areas of the theory include aerospace, automobile, construction and ship-building industries, amongst others. For instance, in the design of a transport aircraft wing, the top and bottom skins, spar webs and ribs are all idealized as plate elements and the dynamic stiffness theory developed above can be exploited when modelling the wing in an accurate and computationally efficient manner. This type of modal analysis is a mandatory requirement in aeronautical design to satisfy airworthiness requirements. The procedure for implementing point or line supports in a structure comprising plate assemblies can be effectively achieved adopting a similar approach given by Anderson et al [39] and any elastically connected coupled structures can also be accommodated, see Liu et al [40]. The proposed theory is versatile and hence can be further developed and interfaced with the finite element method, which will provide an efficient design tool with significant advantages in optimization studies for which an accurate estimation of sensitivities with respect to design variables (structural parameters) is necessary. Importantly, the theory developed can be used as an aid to validate finite element and other approximate methods.

6. Concluding remarks

The application of modified trigonometric basis has been proposed to construct a general solution for the free vibration equations of a thick orthotropic plate leading to the development of its dynamic stiffness matrix. The derived exact solutions are combined in a general series solution. The forms of the solutions made it possible to construct an infinite system of linear algebraic equations connecting the Fourier coefficients of the kinematic boundary characteristics of the plate which are essentially the boundary values of deflections and angles of rotation for the displacement vector and shear forces and

moments for the force vector. Thus, a dynamic stiffness formulation has been realised by connecting the force and displacement vectors to analyze the transverse vibration behaviour of thick orthotropic Mindlin plates for any arbitrary boundary conditions. The theory is demonstrated by several illustrative examples and its validity is further confirmed by comparative results available in the literature.

Acknowledgments

The authors are grateful to the Engineering and Physical Research Council (EPSRC), UK (Grant Ref: J007706) and the RFBR, (Grant Ref: 18-41-920001) which inspired this work.

References

[1] A.J. Keane, W.G. Price, Statistical energy analysis: An overview, with applications in structural dynamics. Cambridge University Press, 1997.

[2] R.H. Lyon, R.G. DeJong, Theory and application of statistical energy analysis, second edition. Butterworth-Heinemann; London, 1995.

[3] F.W. Williams, W.H. Wittrick, Exact buckling and frequency calculations surveyed, J. Struct. Eng., ASCE 109 (1983) 169-187.

[4] F.W. Williams, Review of exact buckling and frequency calculations with optional multi-level substructuring, Comput. Struct. 48(1993) 547-552.

[5] J.R. Banerjee, Dynamic stiffness formulation for structural elements: A general approach. Comput. Struct. 63(1997) 101–103.

[6] W.H. Wittrick, F.W. Williams, A general algorithm for computing natural frequencies of elastic structures, Quar. J. Mech. Appl. Math. 24 (1971) 263-284.

[7] M. Boscolo, J.R. Banerjee, Dynamic stiffness elements and their applications for plates using first order shear deformation theory, Comput. Struct. 89 (2011) 395-410.

[8] M. Boscolo, J.R. Banerjee, Dynamic stiffness method for exact inplane free vibration analysis of plates and plate assemblies, J. Sound Vib. 330 (2011) 2928-2936.

[9] M. Boscolo, J.R. Banerjee, Dynamic stiffness formulation for composite Mindlin plates for exact modal analysis of structures, Part I: Theory, Comput. Struct. 96-97 (2012) 61-73.

[10] M. Boscolo, J.R. Banerjee, Dynamic stiffness formulation for composite Mindlin plates for exact modal analysis of structures. Part II: Results and applications, Comput. Struct. 96-97 (2012) 74-83.

[11] J.R. Banerjee, S.O. Papkov, X. Liu, D. Kennedy, Dynamic stiffness matrix of a rectangular plate for the general case, J. Sound Vib. 342 (2015) 177 – 199.

[12] X. Liu and J.R. Banerjee, An exact spectral-dynamic stiffness method for free flexural vibration analysis of orthotropic composite plate assemblies. Part I: Theory, Compos. Struct. 132 (2015) 1274 – 1287.

[13] X. Liu and J.R.Banerjee, An exact spectral-dynamic stiffness method for free flexural vibration analysis of orthotropic composite plate assemblies. Part II: Applications, Compos. Struct. 132 (2015) 1288-1302.

[14] X. Liu and J.R. Banerjee, A spectral dynamic stiffness method for free vibration analysis of plane elastodynamic problems, Mech. Syst. Sig. Process. 87 (2017) 136-160.

[15] N. Kolarevic, M. Nefovska-Danilovic, M.Petronijevic, Dynamic stiffness elements for free vibration analysis of rectangular Mindlin plate assemblies, J. Sound Vib. 359 (2015) 84–106

[16] M. Nefovska-Danilovic, N. Kolarevic, M. Marjanovic´ M. Petronijevic, Shear deformable dynamic stiffness elements for a free vibration analysis of composite plate assemblies – Part I: Theory, Compos. Struct. 159 (2017) 728–744.

[17] M. Marjanovic, N. Kolarević, M. Nefovska-Danilović, M. Petronijević, Free vibration study of sandwich plates using a family of novel shear deformable dynamic stiffness elements: limitations and comparison with the finite element solutions, Thin-Walled Struct. 107 (2016) 678–694.

[18] S.O. Papkov, J.R. Banerjee, A new method for free vibration and bucking analysis of rectangular orthotropic plates, J. Sound Vib. 339 (2015) 342 – 358.

[19] S.O. Papkov, Vibrations of a Rectangular Orthotropic Plate with Free Edges: Analysis and Solution of an Infinite System, Acoust. Phys. 61(2) (2015), 136-143.

[20] S.O. Papkov, A new method for analytical solution of in-plane free vibration of rectangular orthotropic plates based on the analysis of infinite systems, J. Sound Vib. 369 (2016) 228 – 245.

[21] E. Reissner, The effect of transverse shear deformation on the bending of elastic plates, J. Appl. Mech. 12 (1945) A66–A77.

[22] R.D. Mindlin, Influence of rotatory inertia and shear on fleuxural motion of isotropic elastic plates, J. Appl. Mech. 18 (1951) 31–38.

[23] C.M. Wang, Natural frequencies formula for simply supported Mindlin plates, J. Vib. Acoust. 116 (4) (1994) 536 – 540.

[24] Y. Xiang and G.W. Wei, Exact solutions for buckling and vibration of stepped rectangular Mindlin plates, Int. J. Solids Struct. 41 (1) (2004) 279 - 294.

[25] Y. Xiang and B. Liu, Closed form solutions for free vibrations of rectangular Mindlin plates, *Acta Mechanica Sinica*, 25 (5) (2009) 689-698.

[26] K.M. Liew, Y. Xiang, C.M. Wang, S. Kitipornchai, Vibration of Mindlin plates: programming the p-version Ritz method, Elsevier Science, Oxford, 1998.

[27] D.J. Dawe and O.L. Roufaeil, Rayleigh-Ritz vibration analysis of Mindlin plates, J. Sound Vib. 69 (1980) 345-359.

[28] J.H. Chung, T.Y. Chung, K.C. Kim, Vibration analysis of orthotropic Mindlin plates with edges elastically restrained against rotation, J. Sound Vib. 163 (1) (1993) 151 - 163.

[29] J.H. Chung and D. Zhou, Vibrations of moderately thick rectangular plates in terms of a set of static Timoshenko beam functions, Comput. Struct. 78(6) (2000) 757 - 768.

[30] K.N. Saha, R.C. Kar, P.K. Datta, Free vibration analysis of rectangular Mindlin plates with elastic restraints uniformly distributed along the edges, J. Sound Vib. 192 (4) (1996) 885 - 902.

[31] Y. Xiang, S.K. Lai, L. Zhou, DSC- element method for free vibration analysis of rectangular Mindlin plates, Int. J. of Mech. Sci. 52 (2010) 548 - 560.

[32] K.M. Liew, Y. Xiang, S. Kitipornchai, Transverse vibration of thick rectangular plates – I. Comprehensive sets of boundary conditions, Comput. Struct. 49(1) (1993) 1 - 29.

[33] D. Zhou Vibration of Mindlin rectangular plates with elastically restrained edges using static Timoshenko beam functions with the Rayleigh - Ritz method, Int. J. Solids Struct, 38 (32-33) (2001) 5565 - 5580.

[34] D.J. Gorman and W. Ding, Accurate free vibration analysis of the completely free rectangular Mindlin plate, J. Sound Vib., 18 (3) (1996) 341 - 353.

[35] D.J. Gorman, Accurate free vibration analysis of point supported Mindlin plates by the superposition method, J. Sound Vib. 219 (2) (1999) 265 - 277.

[36] S. D. Yu, W. L. Cleghorn, R. G. Fenton "Accurate Analysis of Free Vibration and Buckling of Clamped Symmetric Cross-Ply Laminates," AIAA J. 32(11) (1994) 2300-2308.

[37] M. Abramowitz, I. A. Stegun, Handbook of mathematical functions, Dover Publications Inc. 1965.

[38] V.T. Grinchenko and V.V. Meleshko, *Гармонические колебания и волны в упругих телах* (Harmonic Vibrations and Waves in Elastic Bodies), Kiev: Naukova Dumka, 1981.

[39] M.S. Anderson, F.W. Williams, C.J. Wright. Buckling and vibration of any prismatic assembly of shear and compression loaded anisotropic plates with an arbitrary supporting structure. Int. J. Mech. Sci. 25(8) (1983) 585-596.

[40] X. Liu, H.I. Kassem, J.R. Banerjee. An exact spectral dynamic stiffness theory for composite plate-like structures with arbitrary non-uniform elastic supports, mass attachments and coupling constraints, Compos. Struct. 142 (2016) 140-154.

Figure(s)

Click here to download high resolution image

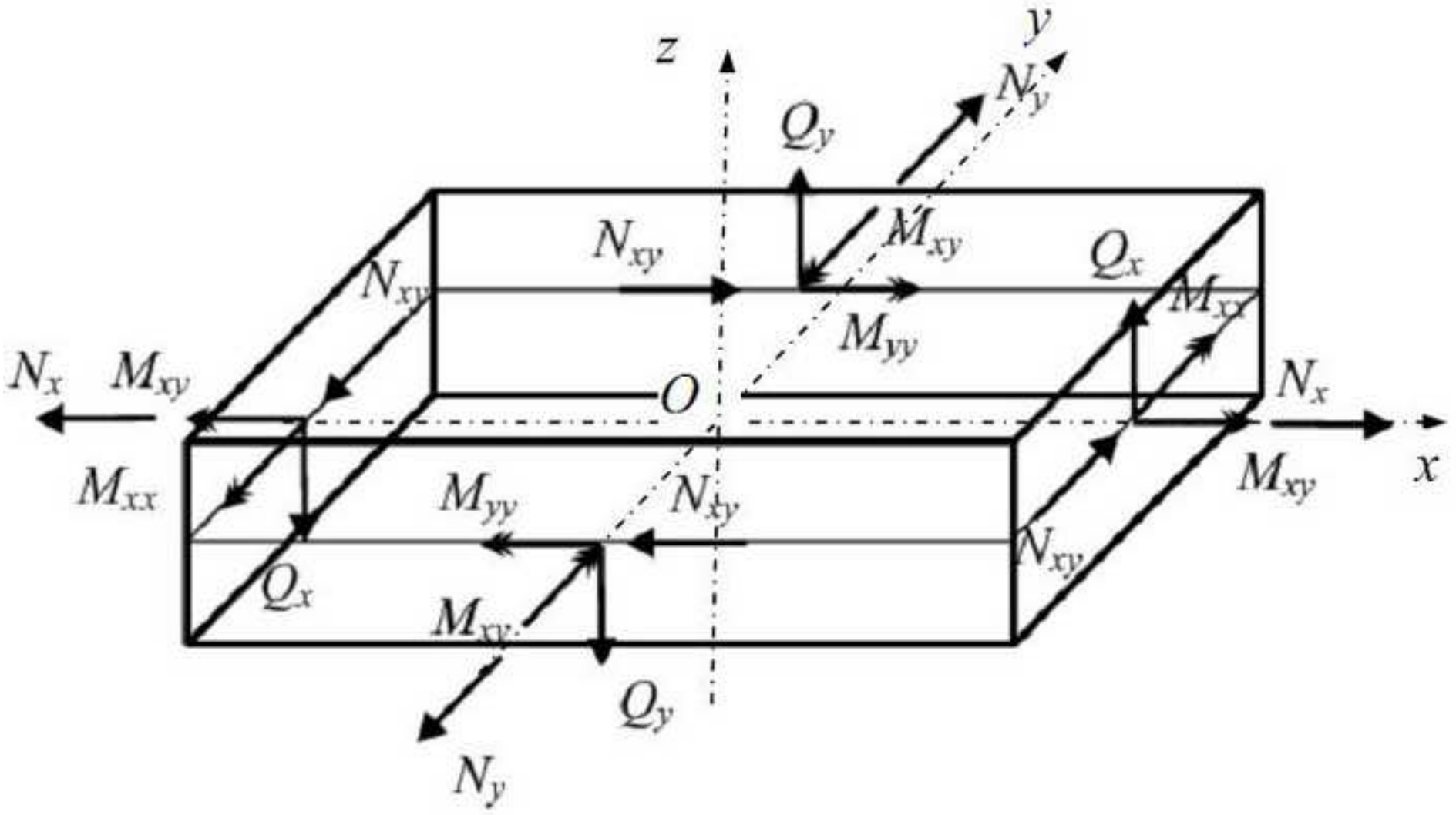

Figure(s)

Click here to download high resolution image

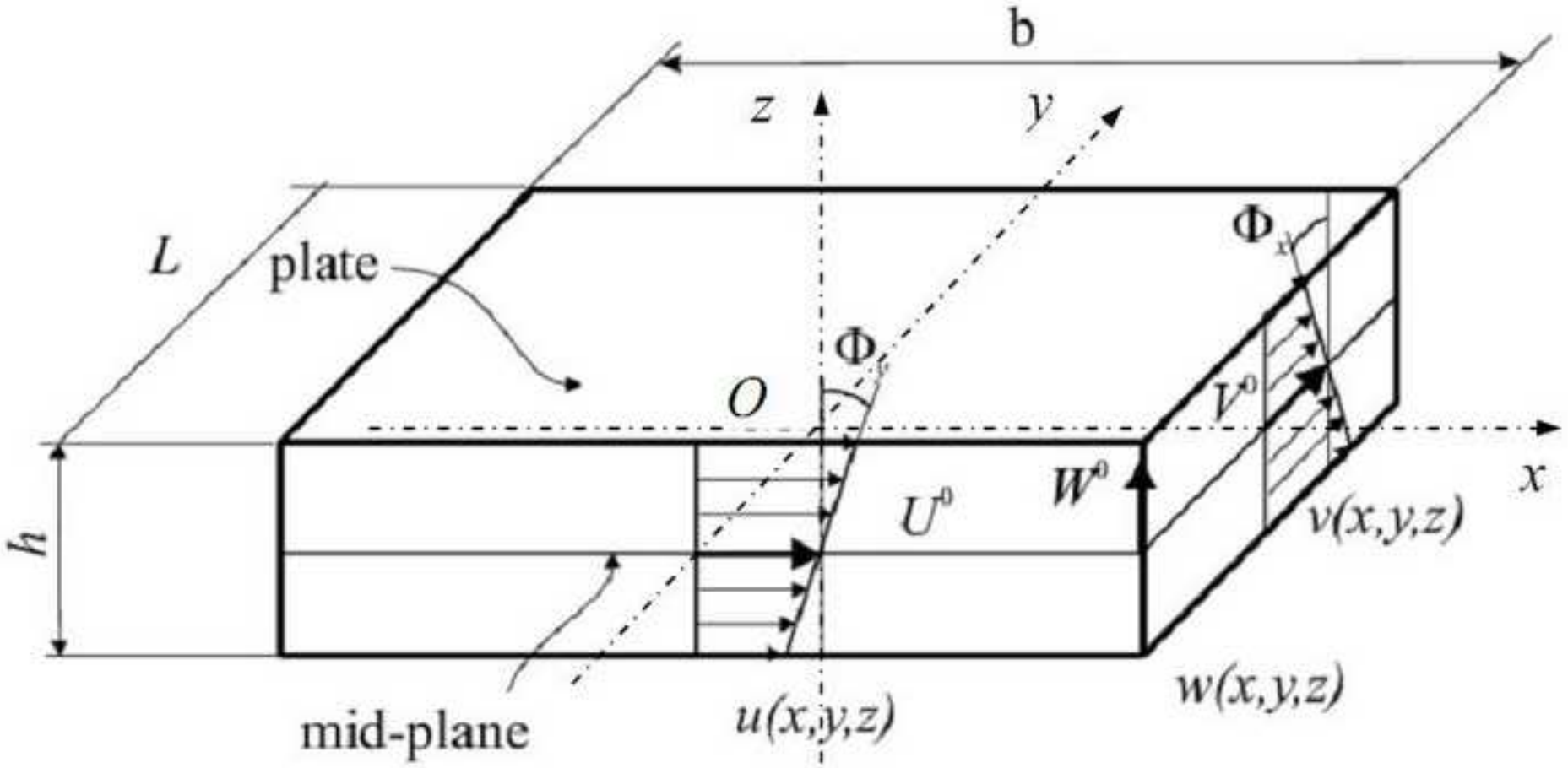

Figure(s)

Click here to download high resolution image

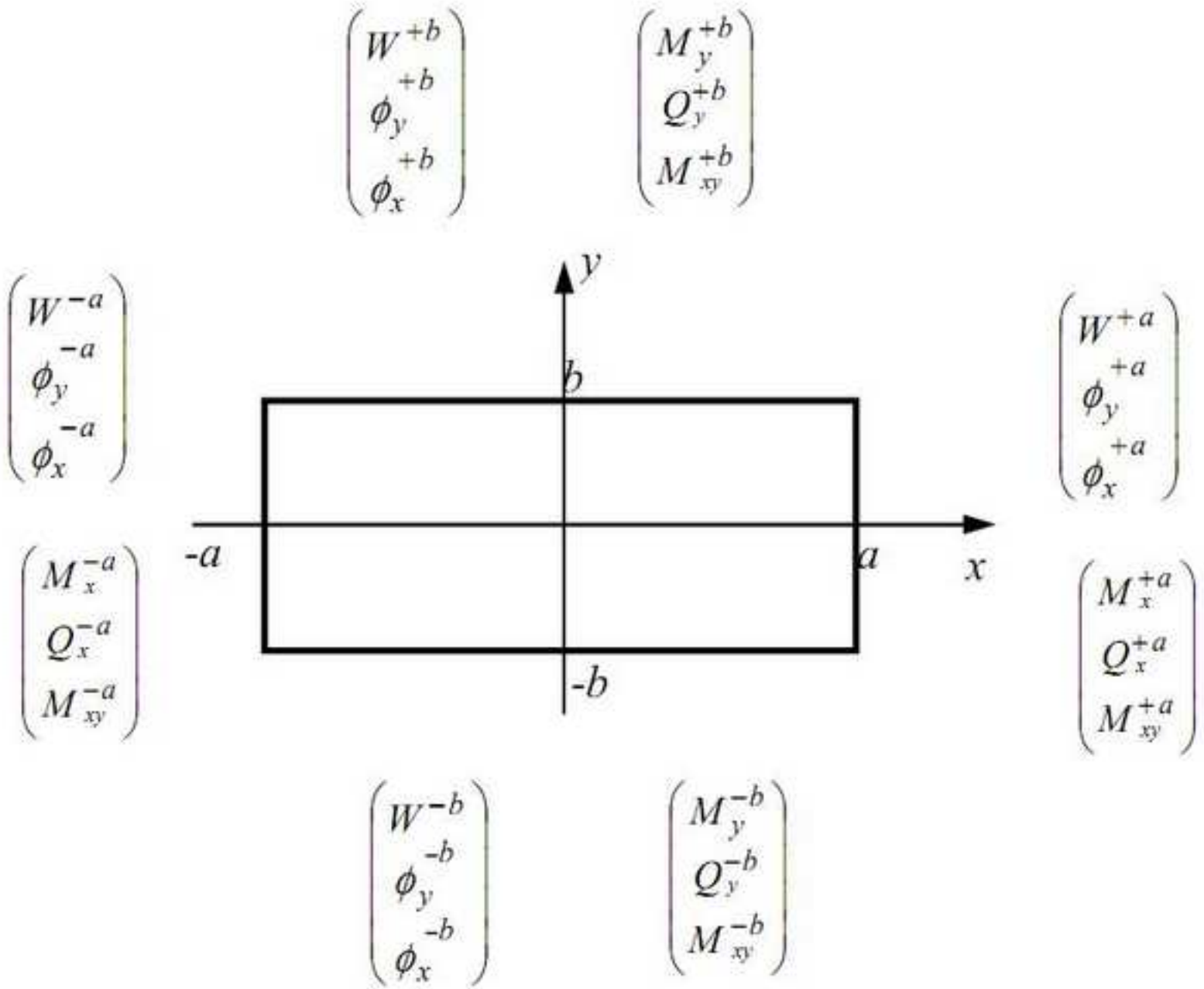

Figure(s)

Click here to download high resolution image

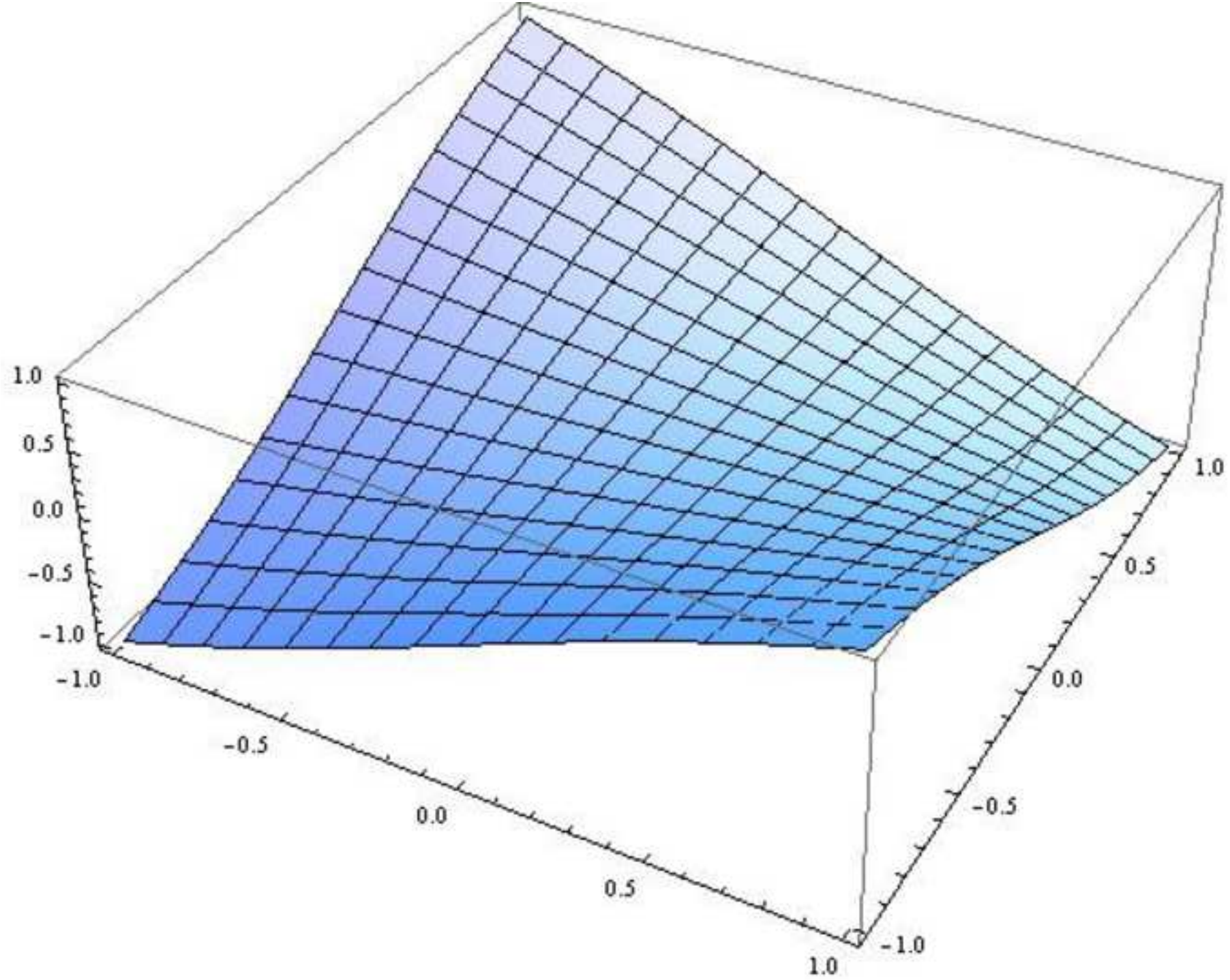

Figure(s)

Click here to download high resolution image

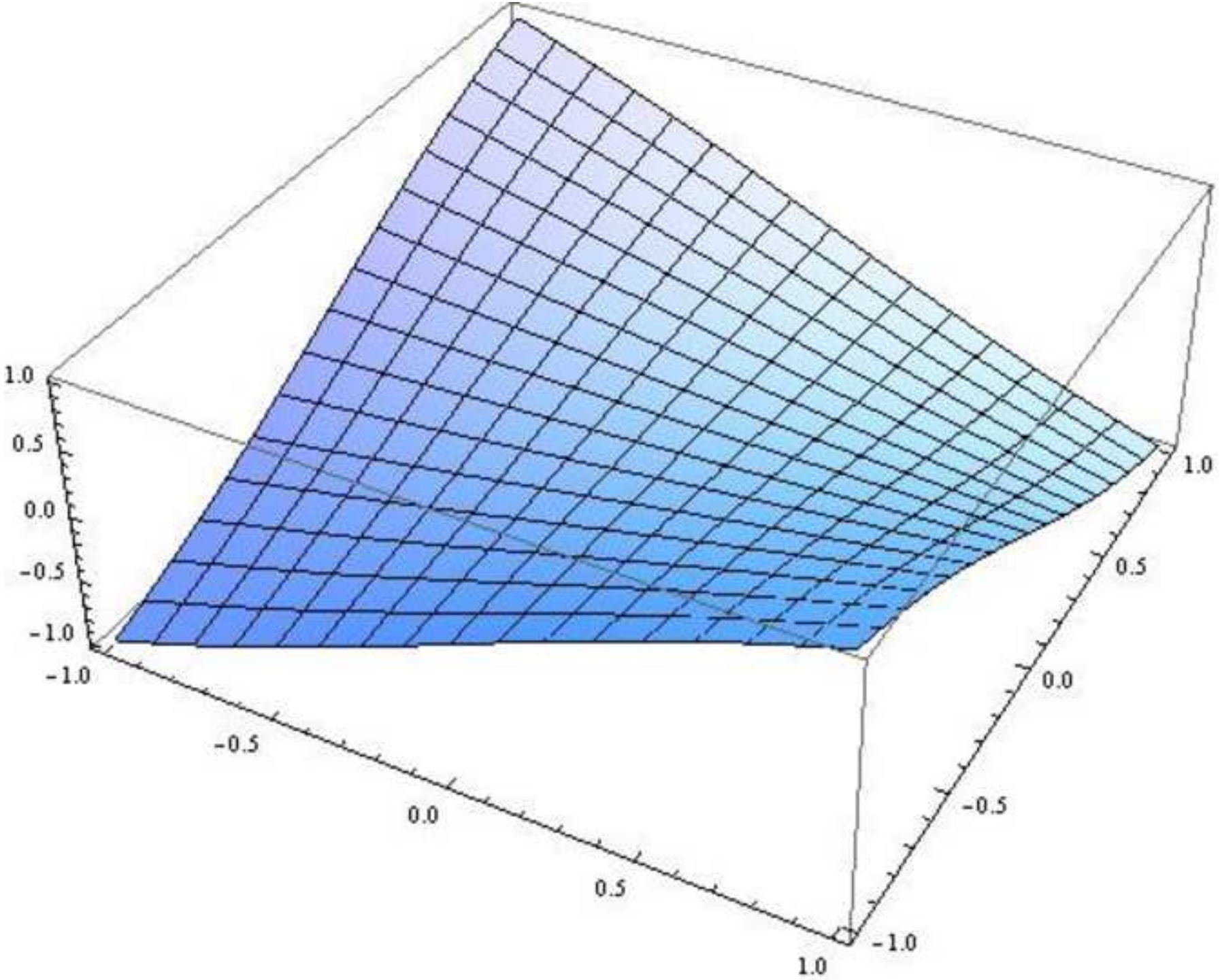

Figure(s)

Click here to download high resolution image

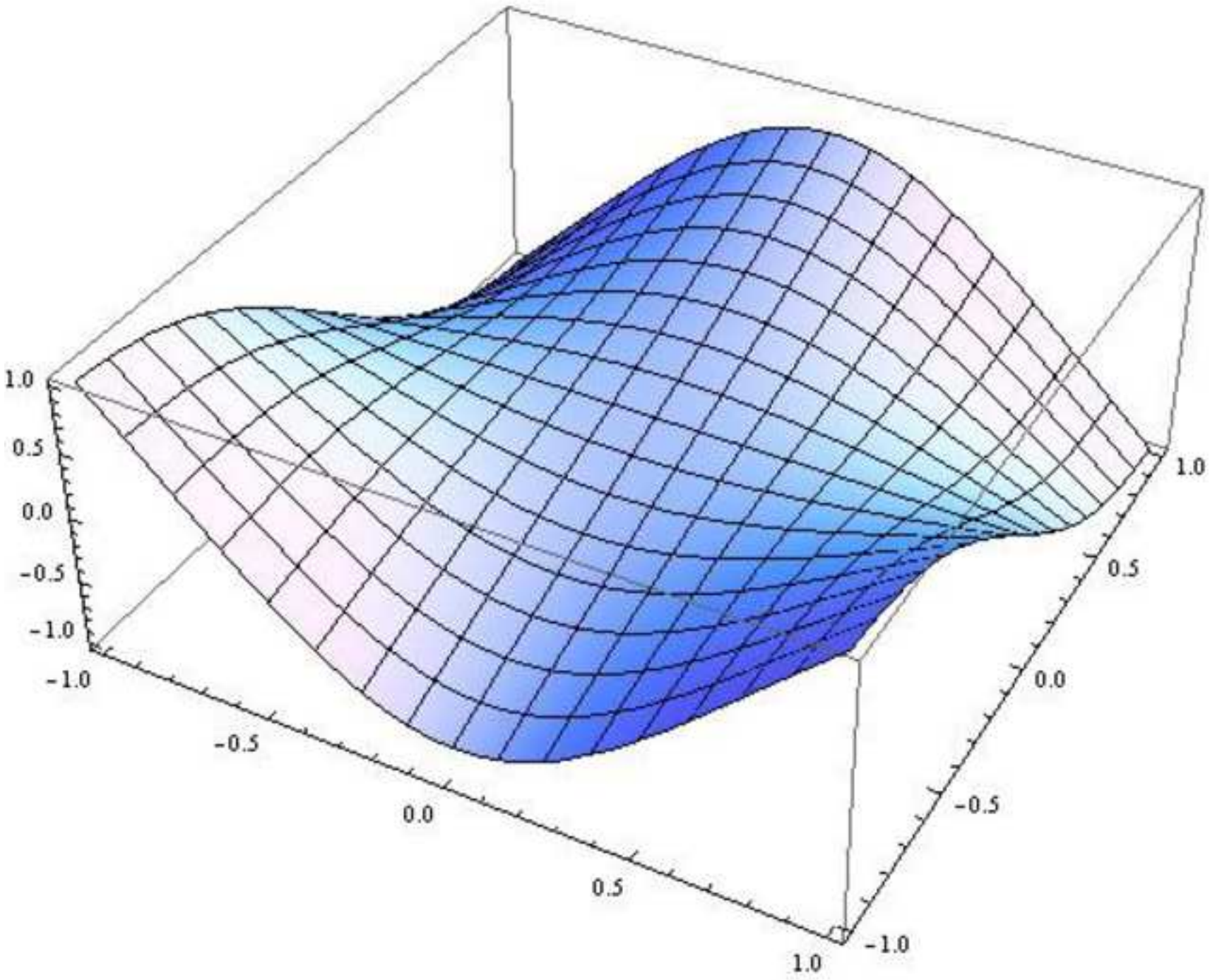

Figure(s)

Click here to download high resolution image

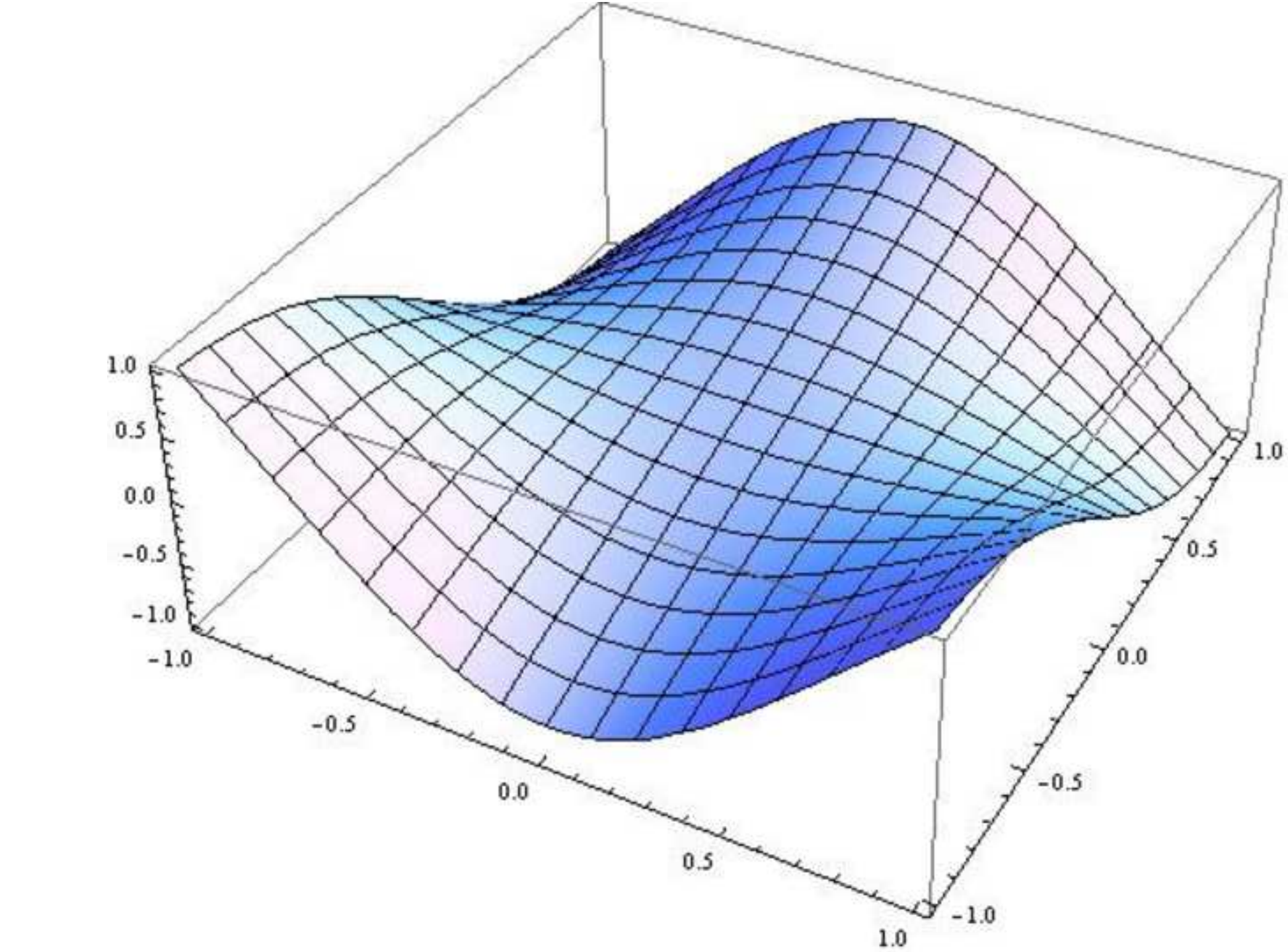

Figure(s)

Click here to download high resolution image

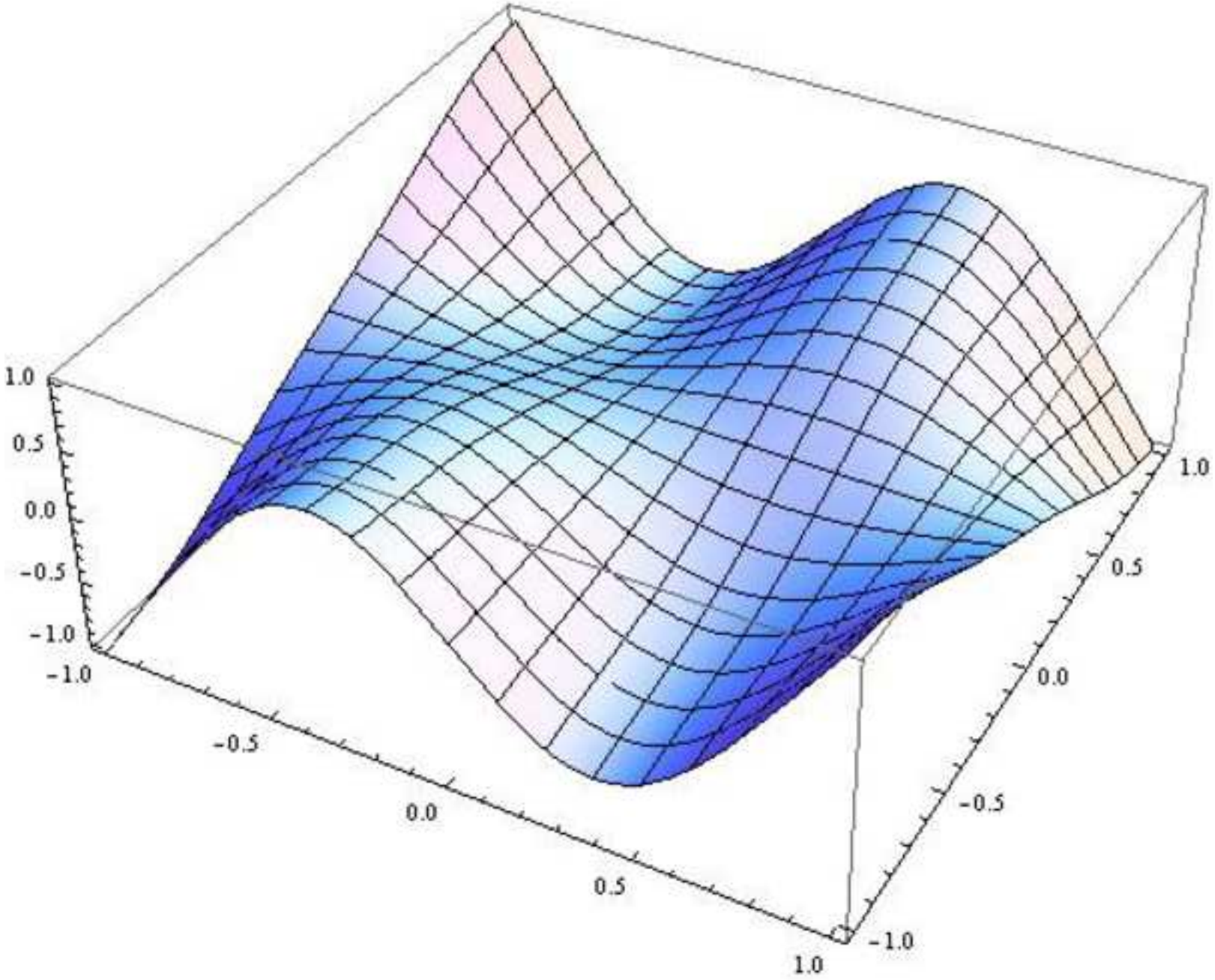

Figure(s)

Click here to download high resolution image

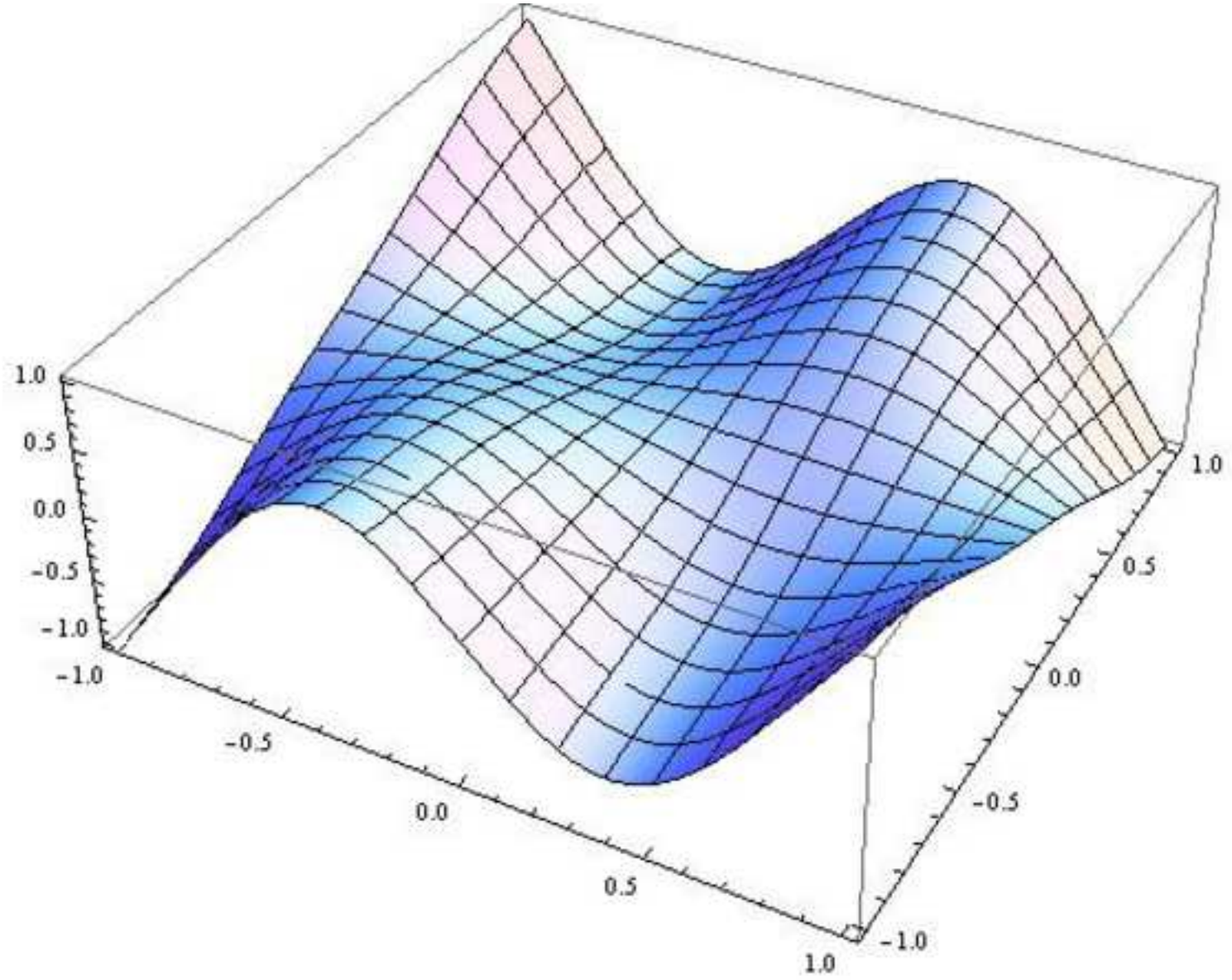

Figure(s)

Click here to download high resolution image

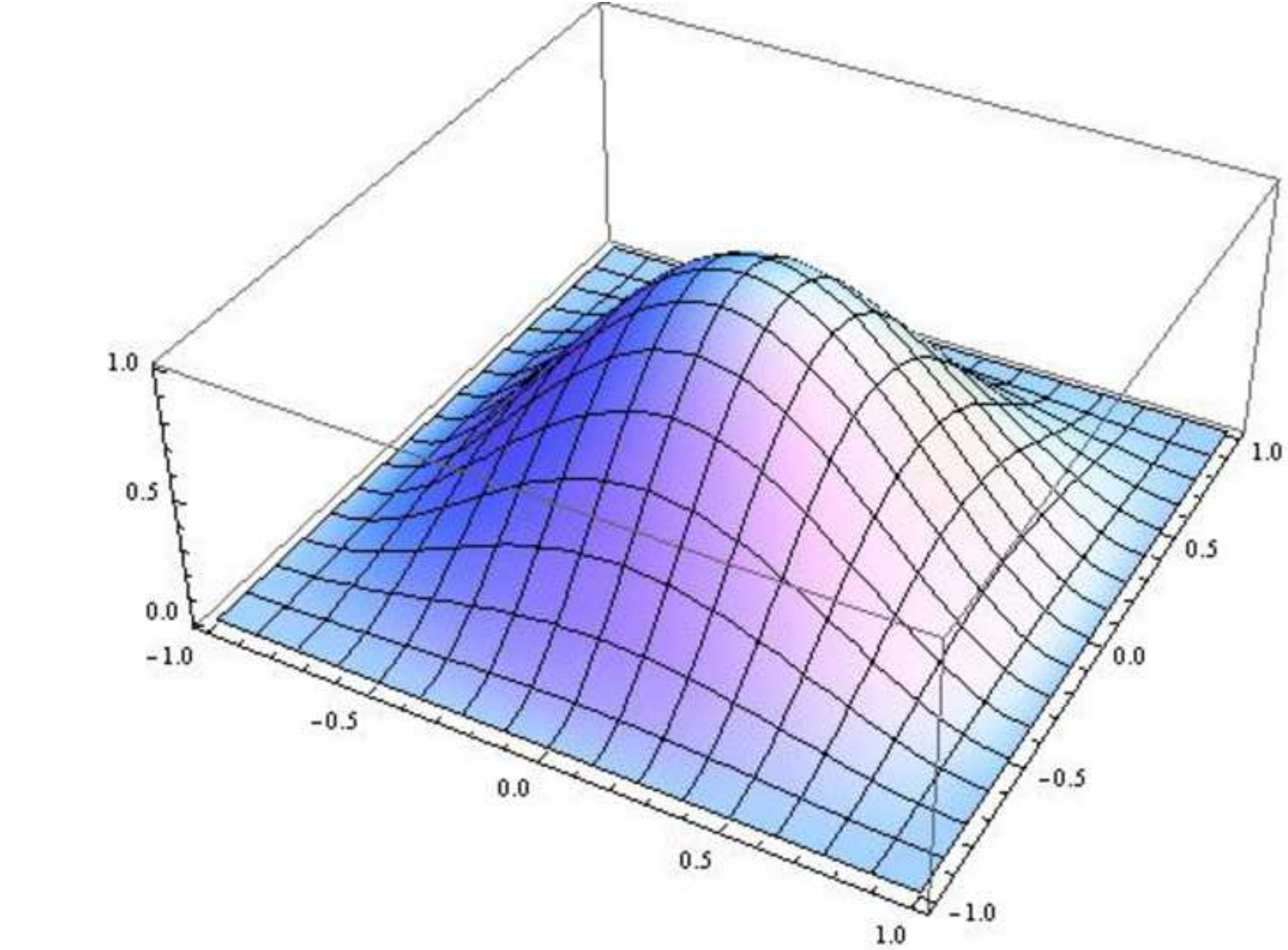

Figure(s)

Click here to download high resolution image

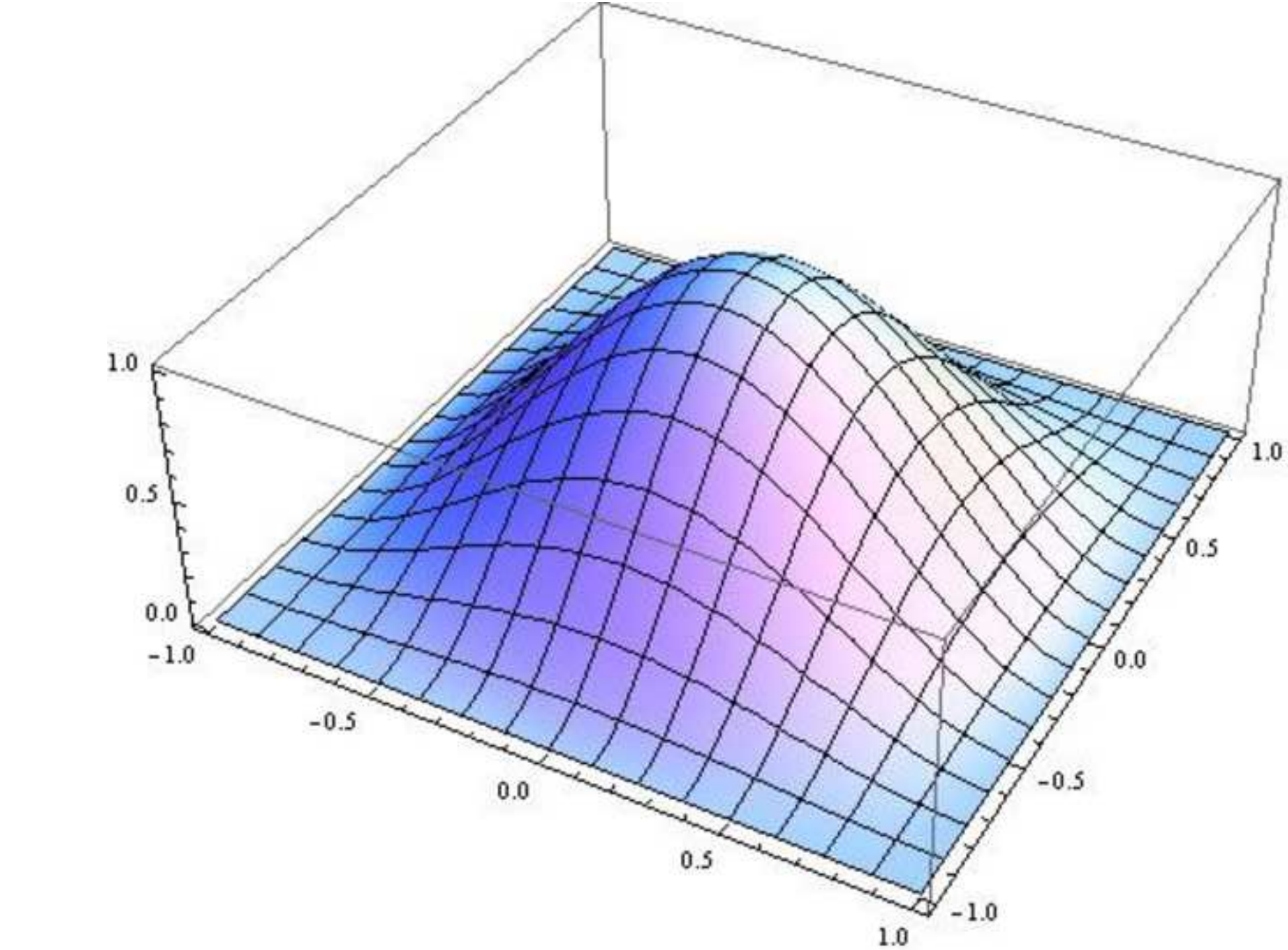

Figure(s)

Click here to download high resolution image

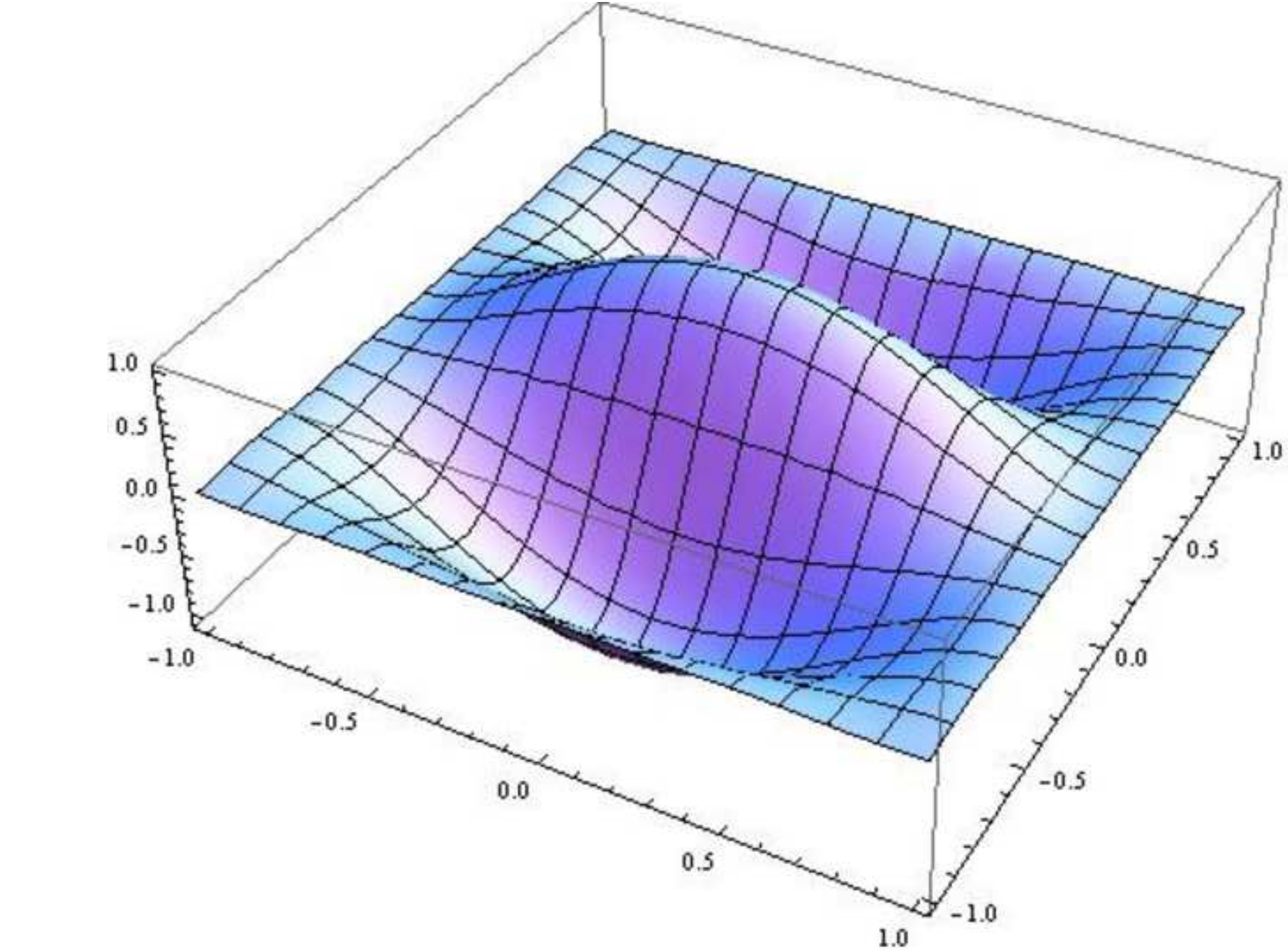

Figure(s)

Click here to download high resolution image

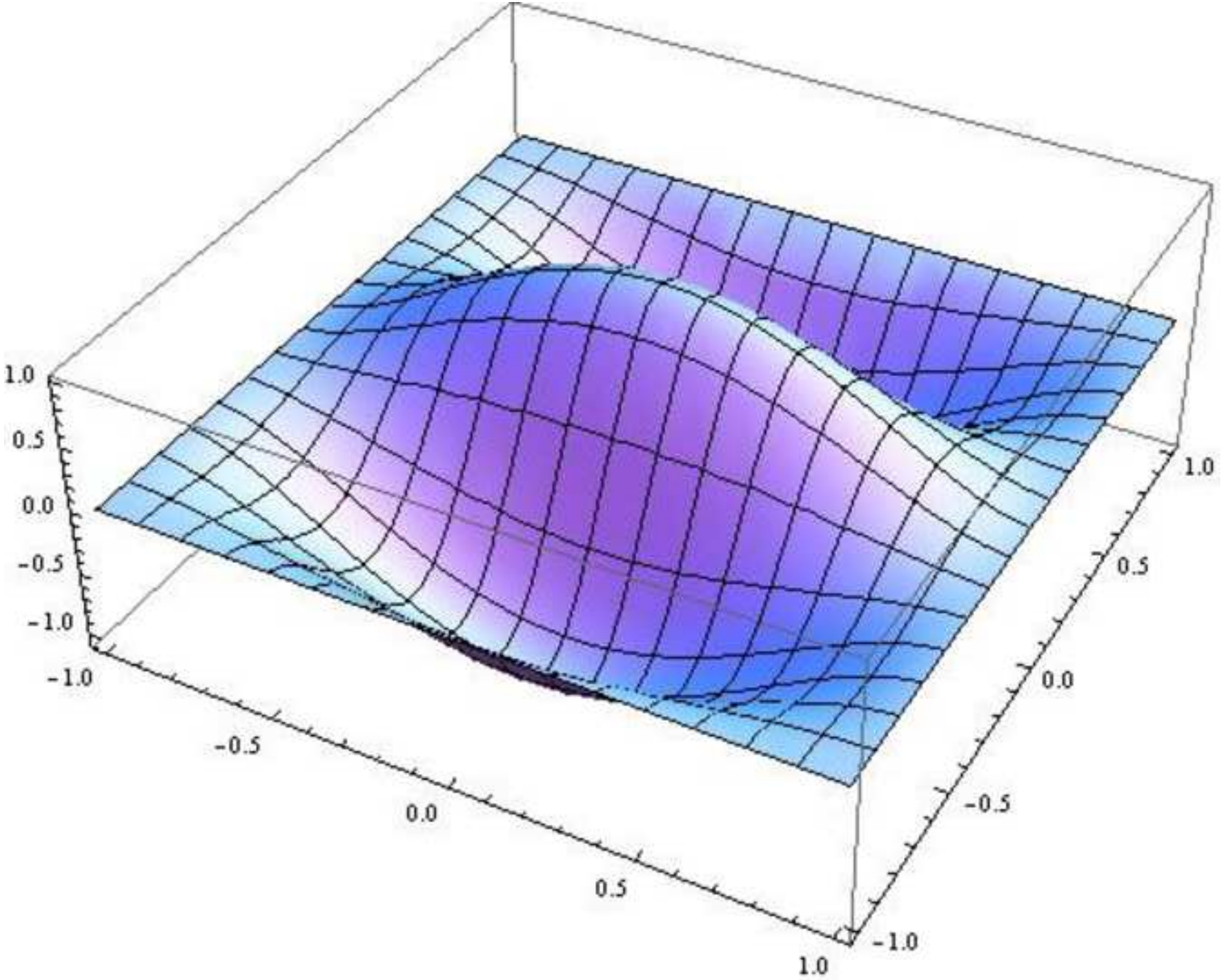

Figure(s)

Click here to download high resolution image

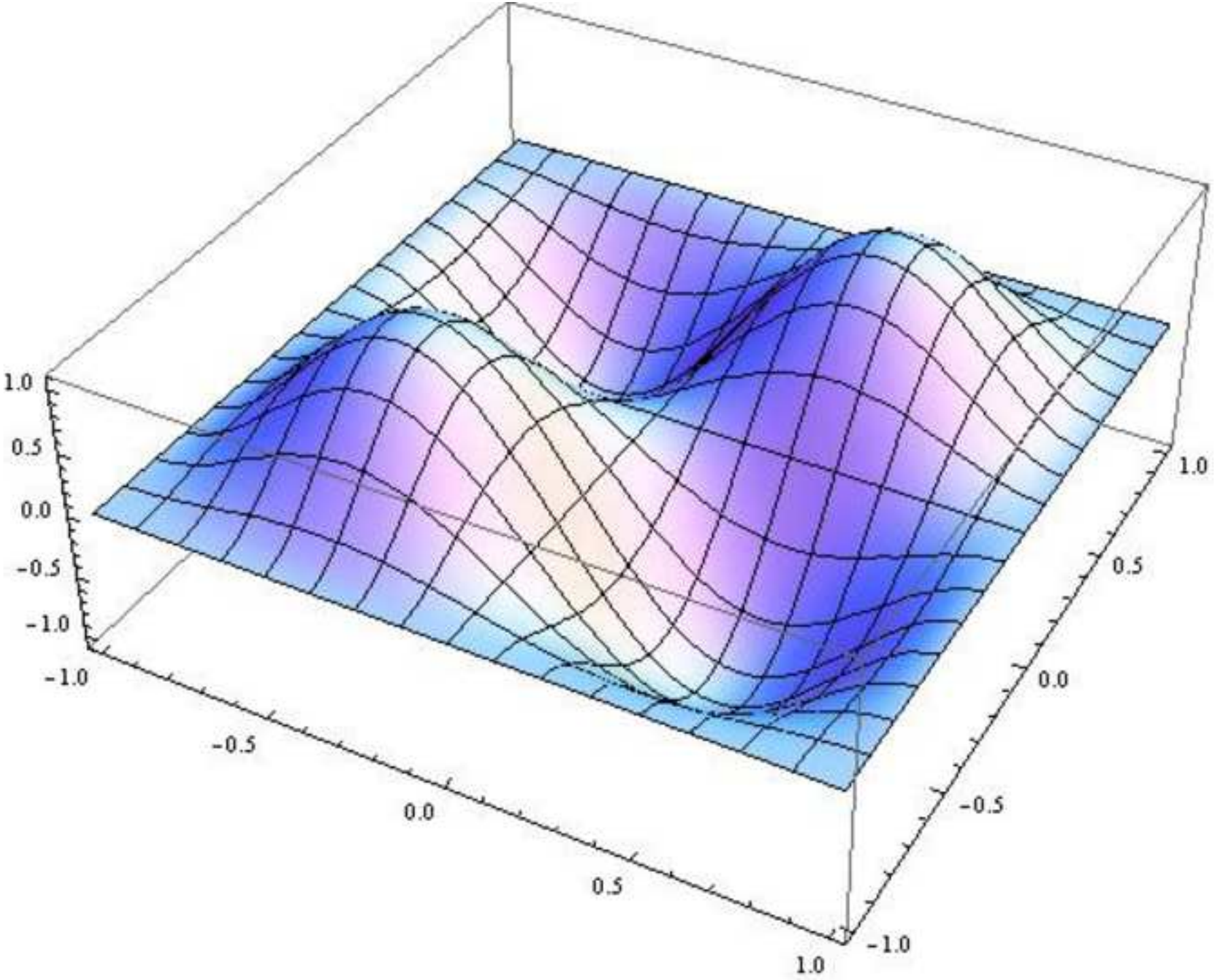

Figure(s)

Click here to download high resolution image

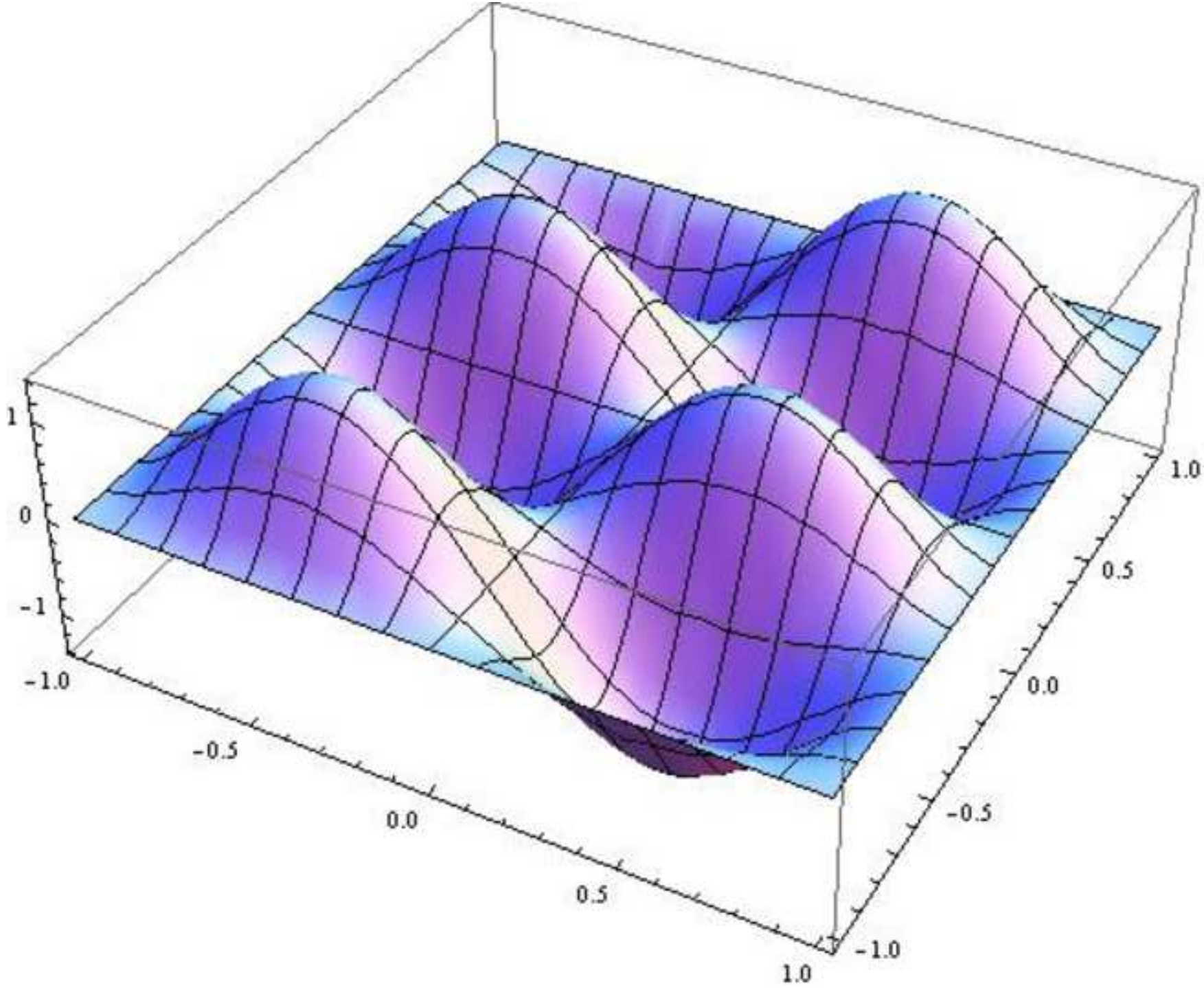

Table(s)

Table 1

The first eight natural frequency parameter Ω for a rectangular isotropic Mindlin plate with FFFF boundary conditions for different values of N; $\nu = 0.333, \kappa = 0.8601, h/a = 0.1, b/a = 3$

Method	Natural frequency and mode sequence number							
	1	2	3	4	5	6	7	8
Symmetry (k, j)	(0,0)	(1,1)	(0,1)	(1,0)	(0,0)	(1,1)	(0,1)	(1,0)
DSM $N = 4$	0.7673	1.0252	1.2781	1.4904	1.8021	1.9053	2.2924	2.3195
DSM $N = 8$	0.7670	1.0248	1.2778	1.4902	1.7910	1.9052	2.2825	2.3162
DSM $N = 16$	0.7670	1.0248	1.2776	1.4902	1.7909	1.9046	2.2814	2.3157
Ref. [34]	0.7657	1.0140	1.2715	1.4715	1.7741	1.8748	2.2494	2.2716

Table(s)

Table 2

Convergence test of fulfilling the zero bending moment requirements when computing the eighth natural frequency ($\Omega = 2.3158$) of a rectangular isotropic Mindlin plate free with FFFF boundary conditions; $\nu = 0.333, \kappa = 0.8601, h/a = 0.1, b/a = 3$

$\frac{y}{b}$	$M_x(a,y)/M_{max}$ N =8	$M_x(a,y)/M_{max}$ N =16	$M_x(a,y)/M_{max}$ N =32	$M_x(a,y)/M_{max}$ N =64
0.0	0.0828	0.0138	0.0013	- 0.0001
0.2	- 0.0468	0.0007	- 0.0019	-0.0006
0.4	- 0.0031	- 0.0168	0.0012	-0.0001
0.6	0.0969	- 0.0045	-0.0015	0.0005
0.8	- 0.1719	0.0368	-0.0008	0.0001
1.0	0.2765	- 0.0096	-0.0083	-0.0053
$\frac{x}{a}$	$M_y(x,b)/M_{max}$ N =8	$M_y(x,b)/M_{max}$ N =16	$M_y(x,b)/M_{max}$ N =32	$M_y(x,b)/M_{max}$ N =64
0.0	0.0000	0.0000	0.0000	0.0000
0.2	- 0.0191	0.0003	0.0000	0.0000
0.4	0.0219	0.0005	0.0000	0.0000
0.6	0.0074	- 0.0005	- 0.0001	0.0001
0.8	-0.0482	-0.0036	0.0005	0.0002
1.0	-0.0428	- 0.0122	- 0.0088	-0.0050

Table(s)

Table 3

The first eight frequency parameters $\tilde{\Omega} = \frac{4\Omega^2}{\pi^2}$ for of a square isotropic Mindlin plate with CCCC boundary conditions for different values of N; $\nu = 0.3, \kappa = 5/6, h/a = 0.1$

Method	Natural frequency and mode sequence number							
	1	2	3	4	5	6	7	8
DSM $N = 4$	3.3020	6.2967	6.2967	8.8211	10.3842	10.4868	12.5645	12.5645
DSM $N = 8$	3.3009	6.2929	6.2929	8.8177	10.3801	10.4826	12.5598	2.5598
DSM $N = 16$	3.3002	6.2926	6.2926	8.8171	10.3793	10.4818	12.5590	12.5590
Ref. [31]	3.2960	6.2873	6.2873	8.8123	10.3791	10.4776	12.5546	12.5546
Ref. [32]	3.2954	6.2858	6.2858	8.8098	10.3788	10.4778	12.5529	12.5529

Table(s)

Table 4

The first eight natural frequency parameters $\tilde{\Omega} = \frac{4\Omega^2}{\pi^2}$ for an isotropic square Mindlin plate with SFSF boundary conditions for different values N; $\nu = 0.3, \kappa = 5/6, h/a = 0.1$

Method	Natural frequency and mode sequence number							
	1	2	3	4	5	6	7	8
DSM $N = 4$	0.9677	1.5785	3.4503	3.7055	4.3580	6.3194	6.7362	7.7817
DSM $N = 8$	0.9562	1.5657	3.4387	3.6920	4.3445	6.3067	6.7152	7.7698
DSM $N = 16$	0.9553	1.5622	3.4355	3.6892	4.3404	6.3019	6.7118	7.7661
Ref. [32]	0.9574	1.5645	3.4328	3.6848	4.3408	6.3006	6.7134	7.7636
Exact results (characteristic equation)	0.9565	1.5593	3.4307	3.6837	4.3358	6.2968	6.7072	7.7645

Table(s)

Table 5

The first eight natural frequency parameters $\tilde{\Omega} = \frac{4\Omega^2}{\pi^2}$ for an isotropic squareMindlin plate with CFFF boundary conditions for $\nu = 0.3, \kappa = 5/6, h/a = 0.1$

Method	Natural frequency and mode sequence number							
	1	2	3	4	5	6	7	8
DSM N = 16	0.3505	0.8170	2.0350	2.5839	2.8621	4.8172	5.4788	5.7741
Ref. [31]	0.3735	0.8403	2.0502	2.5997	2.8752	4.8285	5.4885	5.7860
Ref. [32]	0.3476	0.8168	2.0356	2.5836	2.8620	4.8162	5.4834	57769

Table 6

The first ten natural frequency parameter (Ω_i) for a square glass/epoxy plate with FFFF boundary conditions; $\kappa = 0.8601$ $E_1 = 60.7\,\text{GPa}$, $G_{12} = G_{13} = G_{23} = 12\,\text{GPa}$, $\nu_{12} = 0.23$, $\nu_{21} = 0.094$.

	Natural frequency and mode sequence number									
	1	2	3	4	5	6	7	8	9	10
CPT	1.5832	1.8792	2.3653	2.4872	2.7349	3.1388	3.4892	3.5140	3.9210	4.1395
$h/a = 0.01$	1.5816	1.8793	2.3652	2.4850	2.7331	3.1386	3.4857	3.5115	3.9201	4.1372
$h/a = 0.05$	1.5747	1.8774	2.3615	2.4721	2.7208	3.1298	3.4601	3.4907	3.9014	4.1105
$h/a = 0.10$	1.5643	1.8716	2.3503	2.4490	2.6963	3.1036	3.4095	3.4451	3.8464	4.0427

Table 7

The first ten natural frequency parameter (Ω_i) for a square glass/epoxy plate with CCCC boundary conditions; $\kappa = 0.8601$ $E_1 = 60.7$ GPa，$G_{12} = G_{13} = G_{23} = 12$ GPa，$\nu_{12} = 0.23$，$\nu_{21} = 0.094$

	Natural frequency and mode sequence number									
	1	2	3	4	5	6	7	8	9	10
CPT	2.6975	3.5649	4.1015	4.6283	4.6678	5.4446	5.6157	5.8497	5.9759	6.4397
$h/a = 0.01$	2.6970	3.5567	4.0999	4.6263	4.6662	5.4372	5.6119	5.8203	5.9681	6.4252
$h/a = 0.05$	2.6858	3.5314	4.0634	4.5802	4.6285	5.3761	5.5280	5.7454	5.8719	6.3410
$h/a = 0.10$	2.6527	3.4575	3.9602	4.4539	4.5223	5.2041	5.3035	5.5521	5.6189	6.0943

Table 8

The first ten natural frequency parameter (Ω_i) for a square glass/epoxy plate with CFFF boundary conditions; $\kappa = 0.8601$ $E_1 = 60.7\,\text{GPa}$, $G_{12} = G_{13} = G_{23} = 12\,\text{GPa}$, $\nu_{12} = 0.23$, $\nu_{21} = 0.094$.

	Natural frequency and mode sequence number									
	1	2	3	4	5	6	7	8	9	10
$h/a = 0.01$	0.9363	1.3124	2.1443	2.3484	2.6147	3.2433	3.2674	3.9217	4.1035	4.4660
$h/a = 0.05$	0.9357	1.3080	2.1368	2.3417	2.6021	3.2202	3.2540	3.8955	4.0708	4.4362
$h/a = 0.10$	0.9346	1.2998	2.1212	2.3218	2.5725	3.1693	3.2197	3.8198	3.9877	4.3885

DYNAMIC STIFFNESS FORMULATION AND FREE VIBRATION ANALYSIS OF ORTHOTROPIC MINDLIN PLATES WITH ARBITRARY BOUNDARY CONDITIONS

S.O. Papkov, J.R. Banerjee

Ms. Ref. No.: JSV-D-18-02426

Reply to the reviewers' comments

The authors are grateful to both reviewers for their comments and careful attention to details. Following the reviewers' comments, the paper has now been revised by considering all of the comments made. The paper is without doubt much improved because of the reviewers' comments. In the revised manuscript, all proposed changes are highlighted. A point by point reply to the reviewers' comments is given below Note that the reviewers' comments are shown in italics and the authors' reply in bold.

Reviewer-1

This paper presents an analytical method for free vibration analysis of special orthotropic rectangular Mindlin plates with arbitrary boundary conditions. The manuscript is well written. The work reported should be of interest to the plate vibration community. With some revision, it is publishable in JSV.

The authors appreciate the above comment.

1. *In the reviewer's opinion, the method is based on the two building block technique and the obtainability of the Levy solution for each block. As a result, the proposed method is valid only for special orthotropic rectangular plates with the L-T axes coinciding with the plate edges. If this is the case, the authors should revise the title and make the limitations clear to avoid potential misunderstanding*.

   The authors agree with reviewer that the paper is applicable to specially orthotropic Mindlin plates, not for any arbitrary anisotropic plates. The point made by the reviewer has been taken on board. The authors have now changed the title of the paper by inserting the word "specially" in front of orthotropic.

2. *The half cosine series for an arbitrary function of single variable defined in [0,1] is the same as the modified Fourier series defined in [-1,1]. This can be easily proved through a simple variable transformation*.

   The half cosine series in [0,1] *is* $f(x) = \frac{1}{2}\bar{f}_0^C + \sum_{m=1}^{\infty}\left[\bar{f}_m^C \cos m\,\pi x\right]$

   The modified Fourier series in [-1, 1] *is*

$$f(\zeta) = \frac{1}{2}\hat{f}_0^C + \sum_{m=1}^{\infty}\left[\hat{f}_m^C \cos m\pi\zeta + \hat{f}_m^S \sin\left(m - \frac{1}{2}\right)\pi\zeta\right]$$

   Introducing the following transformation $x = \frac{1}{2}(1+\zeta)$ *into the half cosine series, one can obtain the so-called modified Fourier series*.

   The half cosine series was first used by Gorman in dealing with free vibration of completely free special orthotropic moderately thick (Mindlin) rectangular plates in his book. From this point of view, the proposed analytical solution is not really new.

   The authors are appreciative of the reviewer's well-thought-out observation to highlight the underlying rationale behind the modified Fourier series. It is admitted that Gorman investigated the free vibration problem of a completely free specially orthotropic Mindlin plate using half cosine series, but his approach was somewhat different and rather restrictive, and importantly, his research was not conducted in a dynamic stiffness context, as in the present case. The research described in

the authors' paper has a much wider applicability making it possible to apply the method to complex plate assemblies. It should be noted that one of the main advantages of applying the so-called modified Fourier series is that it allows the investigation to be carried out on any of the component cases of the symmetry. This is possible because of the similarity of expansion into Fourier series of $\cosh t$ with respect to $\cos\frac{\pi n t}{T}$ and expansion of $\sinh t$ with respect to $\sin\frac{\pi(2n-1)t}{2T}$ when $t\in[-T;T]$ (see Eqs. (75) - (78)). In this way, we have used similar expressions for each type of symmetry and later we have combined them together.

3. *The reviewer feels that the way how the boundary conditions are handled in this paper appears and its subsequent reduction to a nonlinear eigenvalue problem for which the W-W algorithm can be used to conduct the eigen-analysis for natural frequencies and mode shapes of rectangular plates with arbitrary boundary conditions*.

   The reviewer is right in his/her assertion that the W-W algorithm has been applied to the developed dynamic stiffness matrix when computing the natural frequencies of the specially orthotropic Mindlin plates. This has now been emphasized in a bit more detail.

4. *With the clear guidance of the superposition, Gorman in his books handled the following challenging aspects in free vibration analysis*:

   - *Interior point or line supports (rigid, elastic or visco-elastic)*
   - *Partial supports on a plate edge (e.g., simple support on one segment and free on the remaining segment)*
   - *Plates of other geometries (trapezoidal, parallelogram, or triangular)*

   Could the authors address comment on the applicability of the proposed approach in addressing one of more of the above.

   The reviewer has made some very important and useful comments which require appropriate reply. The proposed method when suitably adapted can handle rigid or elastic point or line supports, but visco-elastic supports are rather far-fetched and cannot be accommodated at this point of time. Two references have been added ([39] and [40])) which explain how point or line supports can be applied when solving the free vibration problem of isotropic and anisotropic plate assemblies using the dynamic stiffness method. On the question of the second point, the four edges of the plate can have any combination of boundary conditions, namely free, simple-support or clamped. For instance, there can be simple support on one segment or edge of the plate whereas other segments of edges can be free or clamped, see [12-14]. However, on the final point, the authors concede that their method is applicable to rectangular plates only. The theory presented does not cover trapezoidal or triangular plates. This is beyond the scope of the current paper and perhaps this could be the subject matter of future research.

5. *The way how the two Levy solutions are obtained in the manuscript is very similar to the following paper published in 1994*.

   S. D. Yu, W. L. Cleghorn, R. G. Fenton "Accurate Analysis of Free Vibration and Buckling of Clamped Symmetric Cross-Ply Laminates," *AIAA Journal*, 32(11), 2300-2308, 1994.

   The authors are grateful to the reviewer for providing this useful reference which they have now included in their paper.

6. *Minor Typos*

The authors are thankful to the reviewer for his care. All typographical errors have now been corrected. However, in the caption of Fig.2, Plan view is correct and should not be changed to plane view.

Reviewer-2

The authors have carried out a vibration analysis of orthotropic Mindlin plates using the Dynamic Stiffness Method. A new dynamic stiffness formulation is derived based on an extension of the Mindlin theory to orthotropic plates. To my knowledge, the derivations seem correct, and the study is considered original and novel. Therefore, it may be recommended to be published in Journal of Sound and Vibration. However, it is suggested that the authors be required to correct/improve the following points before proceeding with publication.

The authors are encouraged by the reviewer's comment.

1. *Page 12, after Eq. (41), it states "..,X10, X20, Xln and Y10, Y20, Yln (l = 1,2,3;…)", however, in Eq. (25) the suffix l is only 0 or 1. This conflict needs to be clarified.*

   In the expressions for $p_{l,\ nk}$ and $A_{l,\ nk}$ suffix l denoted a branch of the root of the characteristic equation, n corresponds to the trigonometric function $T_k(\alpha_n x)$ and k is the type of symmetry relative to x. Thus, if we consider a special case when the separation constant $\alpha = 0$ then characteristic equation (23) is quartric or bi-quadratic, possessing four roots. However, only two of them give independent terms of the general solution (see Eq. (10)) due to symmetry of the solution, i.e when n=0 we have l = 1, 2. For the general case characteristic equation (13) is of sixth order or bi-cubic, then there exists three independent roots corresponding to l =1, 2, 3 for each value of n. It is recognised that there was a typographical error underneath Eq. (24) which has now been corrected and hence, the reviewer's comment has been addressed.

2. *Page 12, in Eq. (42) coefficients $A_{1,0k}$ and $A_{2,0k}$ are used, whose first suffix conflict with Eq. (25).*

   This comment is directly related to the comment made above and has now been properly addressed so that there is no conflict with Eq. (25) regarding the suffix l.

3. *Eq. (45), "1/D1" in f±a and f±b should be "1/D11"*

   The authors agree with the reviewer. The term D_1 in equation (45) should be D_{11}. Regrettably it was a typographical error which has now been rectified. Thanks to the reviewer for spotting this error.

4. *In Section 5, the results are given for only the cases where the symmetry is are available about the planes through the plate's mid-point. In the paper title, it is mentioned that arbitrary boundary conditions. Therefore, it is suggested to give another result for the case where the symmetry is not available, e.g. a cantilever plate if it is obtainable. If the result is not obtainable the limitation needs to be explained.*

   The authors would like to point out that the symmetry of the rectangular plate has been exploited as a means to an end to obtain the general solution and it is not an end in itself. The symmetric rectangular plate has essentially two planes of symmetry (XZ and YZ planes, leaving aside the XY plane because in-plane displacements are not considered in this paper) so that only one quarter of the whole plate with symmetric-symmetric, symmetric-antisymmetric, anti-symmetric-symmetric and antisymmetric-antisymmetric boundary conditions can be applied on the enforced planes of symmetry giving the solution for the entire plate without any approximation made en route. In this way, the developed dynamic stiffness can be used to compute the natural frequencies and mode shapes of the whole plate for any boundary condition in an exact sense. The authors have now

included an additional set of results for natural frequencies of a cantilever plate, as suggested by the reviewer (see Tables 5 and 8 showing new results)

***Style Checklist**

Journal of Sound and Vibration

Author Checklist

Authors should complete the following checklist and submit with their revised manuscript.

Math notation follows requirements on Guide for Authors (GFA) see: ☒

https://www.elsevier.com/journals/journal-of-sound-and-vibration/0022-460X/guide-for-authors

Use Roman (normal upright) type for: Total differential operators (e.g. d in differential); i or j (square root of -1); exp or e (base of natural logarithms); Re or Im (real or imaginary part); log, ln, sin, cos, etc.; abbreviations such as c.c. (complex conjugate); multiletter symbols (e.g. TL for transmission loss); subscripts of two or more letters identifiable as words or word-abbreviations (e.g., Apipe, fmax) ☒

For more unusual functions, JSV follows Abramowitz and Stegun's book. More detail given in the GFA (see link above).

Unit symbols - These should be upright (e.g. kg, not *kg*). ☒

All authors are listed on the manuscript with correct affiliations, correct email address and are in correct order. ☒

Keywords present. ☒

Manuscript is not currently submitted to any other Journal. ☒

If submitting highlights please note that only six may be submitted and each one should be no longer than 85 characters in length. ☒

Novelty of paper has been clearly stated in the Introduction. ☒

References are presented as per GFA. ☒

References not produced in English language to have English translation in brackets. ☒

Figures and Tables and Equations are numbered in sequence correctly. (See GFA). ☒

Nomenclature (if required) appears on second page of submission. ☒

Acknowledgements should appear in a separate section just after the conclusions. ☒

All abbreviations, in both the abstract and main body of document, are defined once only, the first time they appear in the text. (N.B. The Abstract is treated as an independent text, where references are given in full and abbreviations and symbols, if used, are properly defined.) ☒

Figures – if there are multi-parts to a figures each part is labelled (a) (b) (c) etc. and the labels defined in the figure caption. ☒

Figures – Colour can be used for the on-line version. Figures are reproduced in black and white in the printed journal and must therefore be readable in both colour and black & white. (N.B. charges apply for production of colour figures in the printed journal) ☒

Appendices – should appear before the list of references and labelled A, B, C, (please see GFA for further information regarding equations, figures and tables in the appendices. ☒

Copyright – material reproduced from other publications (e.g. Tables, Figures), source is acknowledged. ☒